PHYSICAL VOLCANOLOGY OF A PYROCLASTIC FLOW

ROTOITI BRECCIA FORMATION, NEW ZEALAND

PHYSICAL VOLCANOLOGY OF A PYROCLASTIC FLOW
ROTOITI BRECCIA FORMATION, NEW ZEALAND

By

Peter J. Fawcett

A Thesis
Submitted to the Department of Geology
in Partial Fulfilment of the Requirements
for the Degree

Bachelor of Science

McMaster University

April 1985

BACHELOR OF SCIENCE (1985)
(Geology)

McMASTER UNIVERSITY
Hamilton, Ontario

TITLE: Physical Volcanology of a Pyroclastic Flow, Rotoiti Breccia Formation, New Zealand

AUTHOR: Peter J. Fawcett

SUPERVISOR: Dr. Paul M. Clifford

NUMBER OF PAGES: vii ; 67

ABSTRACT

The Rotoiti Breccia Formation is a pyroclastic flow deposit located at the northern end of the Taupo volcanic zone, North Island New Zealand. It was formed by a fairly low energy subaerial eruption and subsequent flowage, which restricted it to the topographic low between two older ignimbrites.

Samples from proximal, medial and distal areas fo the flow were examined to determine changes in grain size and particle type distribution as the flow progressed. It was found that on the whole, the flow was very homogenous. However, some initial turbulence at the very beginning of the flow has produced a bimodal grain size distribution presumably due to increased mechanical breakage. A much more prominant crystal population was found in the distal areas of the flow due to rounding of pumice grains and the elutriation of the resultant fines.

ACKNOWLEDGEMENTS

I would like to express my gratitude to Dr. P. M. Clifford for his helpful suggestions and encouragement throughout the year and for allowing me the use of his samples collected from New Zealand. I would also like to thank Dave Collins for his comments and help in solving various problems, and Len Zwicker for his excellent preparation of thin sections.

Finally, I would like to thank my parents for their support and encouragenent over the past four years, and my friends for making them what they were.

TABLE OF CONTENTS

LIST OF FIGURES

LIST OF TABLES

CHAPTER I

INTRODUCTION

During the year 1979/1980, P.M. Clifford did extensive collecting of pyroclastic flow material from the Rotoiti Brecca Formation, North Island, New Zealand. In all, over 200 samples from all parts of the flow were collected. From these, 18 samples were selected as representative of the different areas of the flow and incorporated into this study.

This study is concerned with the physical volcanology of the pyroclastic flow, specifically with determining the types of processes involved in emplacing the final deposit and their extent. It involves comparisons of grain size distributions, component analyses and grain shapes between proximal and distal areas of the flow. Also both phenocrysts and pumice fragments are examined in order to determine conditions in the magma prior to the eruption.

1. PHYSICAL VOLCANOLOGY OF PYROCLASTIC ROCKS

Pyroclastic rocks are the products of explosive subaerial or subaqueous eruptions and are manifested particularly as pyroclastic flow deposits (ignimbrites) and as air-fall deposits.

Air-fall deposits are formed when the fragments produced by an eruption are transported through the air either by ballistic trajectory for larger sizes or turbulent suspension for smaller sizes and fall back to the ground. The resulting deposit is a layer of volcanic ash draped uniformly over the underlying topography in layers which thin distally. Individual layers show normal or reverse grading and moderate to good sorting of their particulate constituents. Fall out deposits are also formed by very fine grained material elutriated by hot gas from a moving pyroclastic flow.

Pyroclastic flows are hot gaseous particulate density currents created when the material produced by an eruption is too dense to become airborne. The deposits formed by these flows are quite diverse reflecting different eruptive styles and depositional regimes (Fisher and Schminke, 1984) and are nowadays generally termed ignimbrites. The term ignimbrite was first used by Marshall (1935) to describe a pyroclastic rock in New Zealand whose constituents were welded together by a high heat flow. Ignimbrite is now used to describe any pyroclastic flow deposit, welded or non-welded.

Pyroclastic flows originate by gravitational collapse of vertical eruption columns, low pressure boiling over of a magma from a vent or by a laterally directed blast (as in the May 19th, 1980 Mt. St. Helens eruption) which is usually associated with the formation or collapse of a lava dome.

Pyroclastic flows are extremely mobile and move at high velocities. Depending on the terrain, travel distances of a single unit over 100 km. are not uncommon, e.g. the Taupo Ignimbrite (Walker et al, 1981). The flows move over and around obstacles, over low gradients and even uphill for short distances. Higher areas will 'drain' into topographic lows so the thickness of a flow unit will vary locally and may be stratigraphically discontinuous with its source if the source is elevated. This will also tend to produce a flat upper surface on the flow.

This extreme mobility is largely due to the partly fluidized nature of a flow. The exsolution of hot gas from the magma derived particles as well as entrained atmospheric gas bouys up smaller fragments which in turn reduces the internal friction of the entire flow. This internal lubrication system allows the entire mass of material to be easily acted on by gravity even on a shallow slope. Another possible explanation for the mobility of pyroclastic flows is the kinetic energy imparted to a flow by the gravitational collapse of an overloaded eruptive column. If a collapse were to occur between 5 and 10 km. above a vent, the resulting debris would travel the same distance unfluidized as a fluidized flow without this extra kinetic energy (Sparks 1976). However, as these eruptive conditions do not exist for all ignimbrites, this extra kinetic energy is minor in importance compared to fluidization.

Pyroclastic flow deposits contain a wide range of clast sizes and so are poorly sorted with values of $\sigma\phi$ (Inman parameters) greater than 2.0. Sparks (1976) suggests that high particle concentration rather than turbulence gives a flow the capacity to carry large clasts and results in the poor sorting found in ignimbrites. Sorting values tend to decrease with increasing length of transport (Sheridan, 1971, Walker, 1971, and Sparks, 1976). The sorting of an entire deposit is partly dependent on the relative abundances of its constituents--pumice, lithics, and crystals--as these subpopulations may differ in their sorting for reasons other than eruption and transport processes.

For example, the size distribution of crystals depends on the amount of crystallization in the magma prior to eruption and the amount of breakage during eruption. Lithics can be derived from the vent or magma chamber walls or be picked up by a flow as it moves along the ground, and so give rise to very local anomalies in abundance and size distribution patterns.

Pumice is formed by the rapid quenching of a magma upon eruption, freezing in exsolved gas to produce vesicles. Previously formed crystals are also incorporated into pumice layers, but they may be freed by pumice breakage. The same breakage yields the abundant glass shards found in an ignimbrite. The most prominent crystal types are quartz, sanidine, and plagioclase with minor amphibole, pyroxene, biotite, and Fe/Ti oxide (Fisher and Schminke, 1984) which crystallize to different forms and therefore may be separated from each other. Quartz is the most dominant phase, thus rhyolite is the most important rock type forming large ignimbrite sheets.

The material which characterizes the final deposit differs somewhat from the primary erupted material. Breakage of pumice liberates crystals and generates shards (noted above). Many of these shards are swept up and out of the flow itself to form the dust laden, highly turbulent cloud above the ground hugging flow. Pictures of the Taal eruption of 1965 and of Ngauruhoe, 1974, show such supra-fine clouds. The loss of these shards causes an enrichment of crystals in the flow while contributing to the airfall deposits.

Pyroclastic flows are on the whole very homogenous. However, in the distal portions of a flow, some vertical grading may be present. Pumice clasts are commonly reversely graded (Sparks, 1976) while lithic fragments are normally graded (Sparks et al, 1973), though the reverse of the above cases have also been found. The basal layer of an ignimbrite is commonly fine grained, which results from two processes. Fragments with a higher density will tend to fall towards the bottom of a flow under the influence of gravity. Also, the high concentration of clasts in a flow acts as a sieve allowing only smaller particles to fall through. Thus, pumice fragments may be three times larger at the top of a flow than at the base (Kuno et al, 1964). In subaerial deposits, the maximum size of both lithics and pumice decreases with distance, though usually not very rapidly (Kuno et al, 1964).

Figure 1. The Taupo Volcanic Zone, North Island, New Zealand. (1) Rotorua Caldera (2) Okataina volcanic centre (3) Maroa volcanic centre and (4) Taupo volcanic centre

(Nairn and Kohn, 1973)

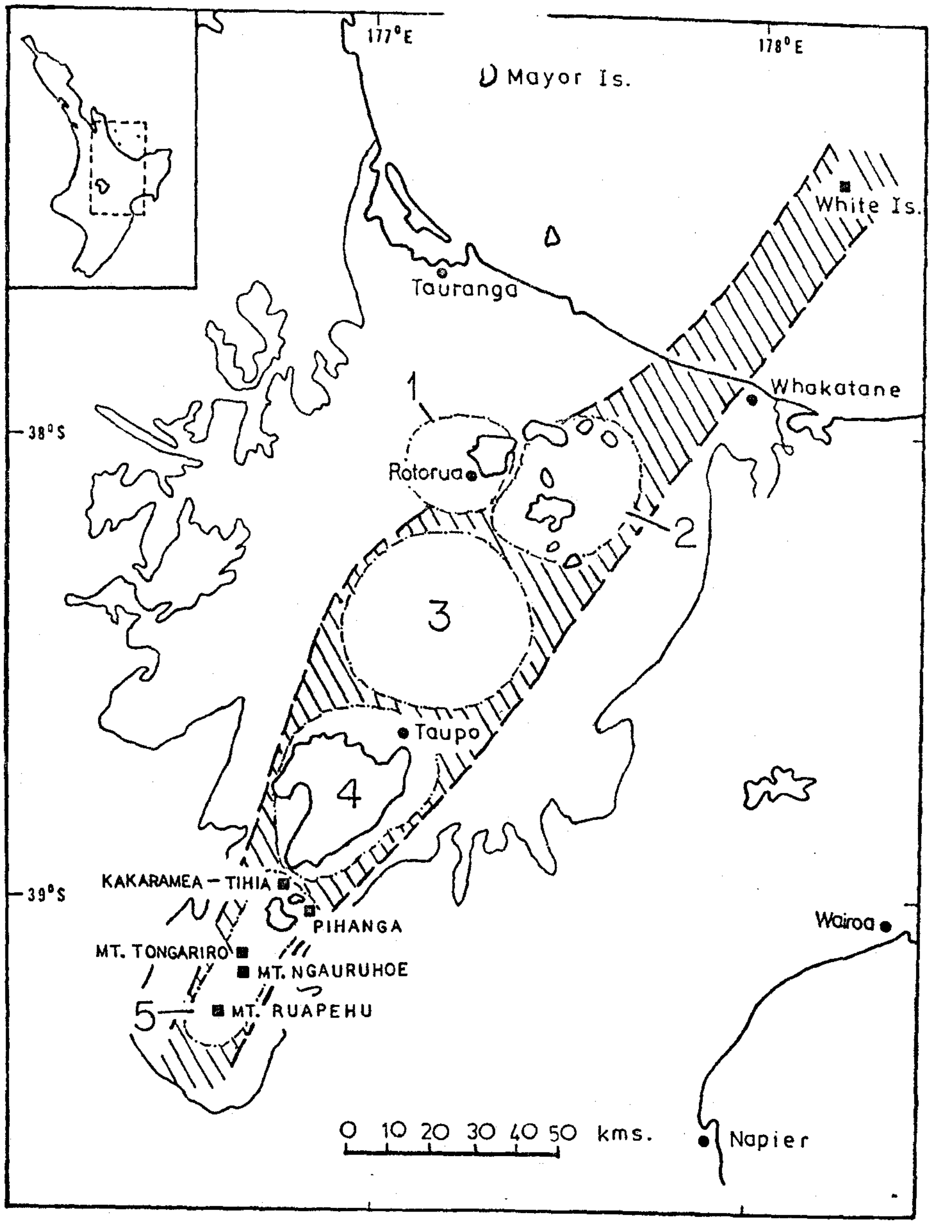

177°E
178°E
Mayor Is.
White Is.
Tauranga
Whakatane
38°S
Rotorua
1
2
3
4
5
Taupo
KAKARAMEA – TIHIA
39°S
PIHANGA
MT. TONGARIRO
MT. NGAURUHOE
MT. RUAPEHU
Wairoa
0 10 20 30 40 50 kms.
Napier

Figure 2. Map of the Rotoiti Breccia Formation and surrounding formations. Samples are shown in their approximate locations.

M	Mesozoic Sediments
Ma	Matahina Ignimbrite
Mk	Mamaku Ignimbrite
Ok	Okataina Volcanic Centre
Rb	Rotoiti Breccia

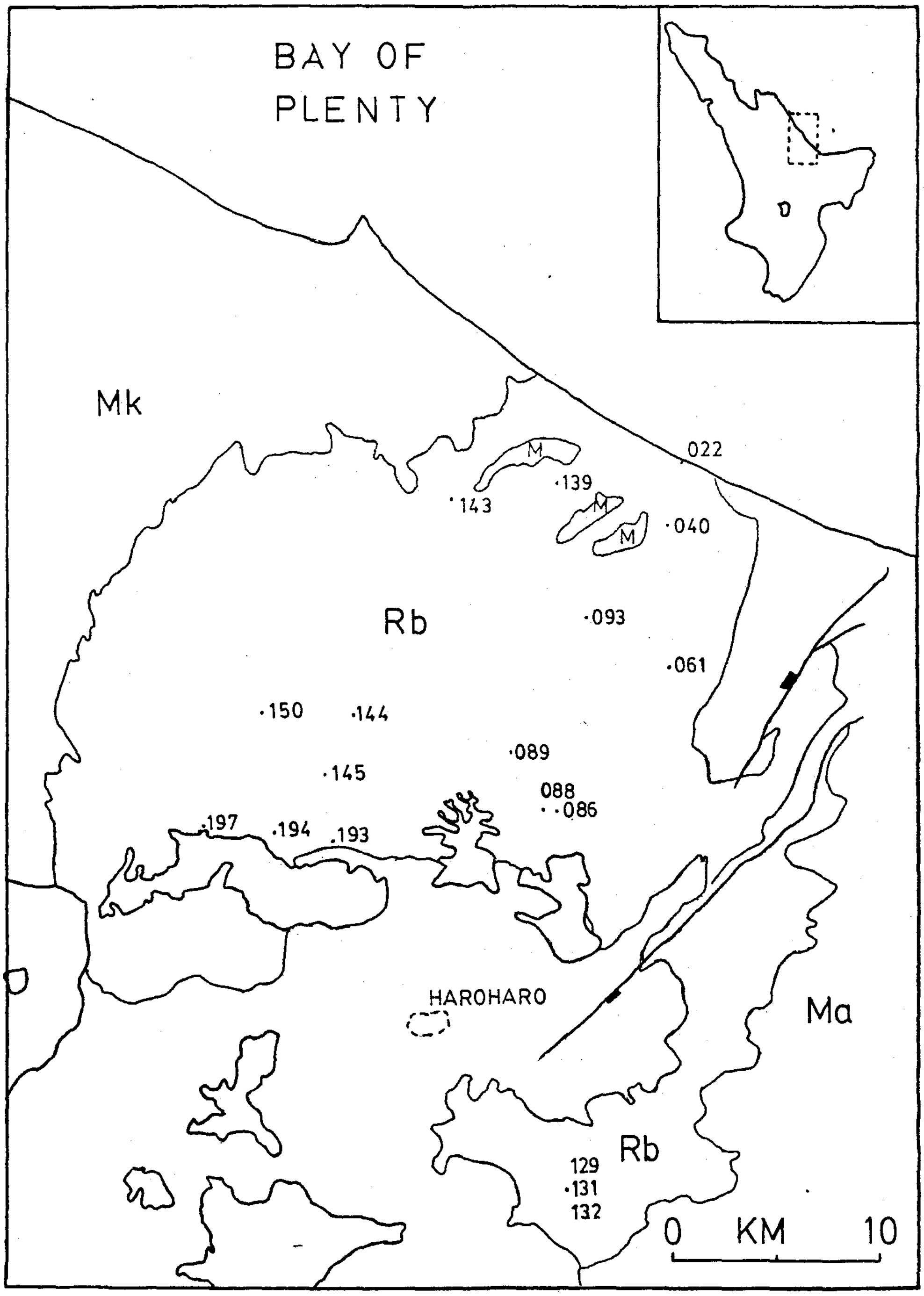

BAY OF PLENTY
Mk
M
M
M
022
·139
·143
·040
Rb
·093
·061
·150
·144
·089
·145
088
· ·086
·197
·194
·193
HAROHARO
Ma
Rb
129
·131
132
0 KM 10

CHAPTER II

GENERAL GEOLOGY

1. THE TAUPO VOLCANIC ZONE

The Taupo Volcanic Zone is an area of Pleistocene to recent calc-alkaline volcanism on the North Island of New Zealand. It extends northeastward from Mt. Ruapehu in the south to White Island in the Bay of Plenty, a total length of 250 km. On average, its width is 30 km. with a maximum width of 50 km. It is both a structural and topographic low, controlled by a series of northeast trending faults.

The dominant volcanic type is rhyolite which occurs as lavas and domes, large extents of welded ignimbrites, and unwelded pumice breccias (of which the Rotoiti Breccia is an example), and as blanketing pumice air fall deposits. Andesites are found at the extreme ends of the zone only; on White Island and in the Tongauro volcanic centre to the south. Basalts, as at Tarawera, and dacites are found in the zone, but are volumetrically small compared to the rhyolites.

The rhyolite volcanism has been largely concentrated in five centres; the Taupo volcanic centre, the Maroa volcanic centre, the Tongauro volcanic centre, the Okataina volcanic centre, and the Rotorua Caldera (see Figure 1). Each centre is defined by a concentration of rhyolite domes and is flanked by extensive ignimbrite sheets. Gravity and magnetic anomalies show ring structures at depth for each centre which are interpreted as collapse features resulting from large-scale magma withdrawal from the upper crust (Rogan, 1982). A very generalized sequence of eruptions for each centre has been proposed by Ewart and Stipp and is as follows: (1) ignimbrite eruptions, (2) the extrusion of viscous rhyolite domes around the periphery of the centres, (3) localized glowing avalanche eruptions depositing partly welded or unwelded pumice breccias, (4) a resurgent phase of rhyolite doming and flows, usually within the central areas of the volcanic centres, and (5) violent ash-fall eruptions which blanket the region with pumice air-fall deposits (Ewart and Stipp, 1968).

The rhyolitic magmas were probably derived by widespread partial fusion of the upper crust (mainly eugeosynclinal greywacke-argillite sediments) as such an origin is consistent with the rhyolites' main chemical and mineralogical characteristics (Ewart and Stipp, 1968). The same authors have carried out a major element analysis of lavas and ignimbrites in the area which show a very high amount of SiO_2 and thus are definitely rhyolite (see table 3).

2. THE ROTOITI BRECCIA FORMATION

The Rotoiti Breccia Formation is a rhyolitic pyroclastic flow of upper Pleistocene age which was extruded at the northern end of the Taupo Volcanic Zone. The great bulk of it extends north-eastwards from the Lake Rotoiti-Lake Rotoma area to the Bay of Plenty and part fringes the Okataina Volcanic Centre to the east and west. The Rotoiti Breccia is considered to have been erupted from the Okataina

Volcanic Centre, specifically the Haroharo Rhyolite Complex (Nairn and Kohn, 1973) (See fig.2). It overlies the Mamaku Ignimbrite to the west and the Matahina Ingimbrite to the east. The contact between both these ignimbrites is presumed to underly the Rotoiti Breccia and the Rotoiti Breccia occupies the topographic low where these ignimbrites meet. In a few places, rivers and streams have cut through the formation to expose the underlying ignimbrites. To the north, three 'islands' of Mesozoic sediments are found around which the pyroclastic material moved. It does not appear that the flow ever covered the tops of these (Clifford, personal communication).

The Rotoiti Breccia consists of unwelded pumice flows locally interstratified with a series of shower-bedded ash deposits collectively known as the Rotochu Ash (Nairn, 1972). One such airfall sequence forms the basal unit to the formation (see tab 1). The other airfall sequences are locally distributed within the Rotoiti Breccia, but their great bulk is found outside the flow deposit's range. There is no significant time interval between the eruptions of the Rotochu Ash and the pyroclastic flows, the Rotochu being regarded as a pre-flow product of the eruption. By using isopachs generalized from Vucetich and Pullar (1969), Nairn (1972) determined that approximately equal volumes of airfall tephra and pyroclastic flow material (50 cubic km. each) were erupted. The entire formation was erupted in a short period of time and possibly represents a single cooling unit (Nairn, 1972).

Two dates have been determined for the Rotoiti Breccia Formation by radiocarbon methods used on charcoal samples found at the base of the Rotoehu Ash; 41,600 years B.P. (Thompson, 1968) and 44,200 ± 4,300 years B.P. (Grant-Taylor and Rafter, 1971).

TABLE 1

PYROCLASTIC STRATOGRAPHY OF ROTOITI BRECCIA FORMATION

(Nairn, 1972)

LITHOLOGY	FORMATION	
	Rotorua Subgroup	
	Okareka Ash	
	Te Rere Ash	
	Oruanui Ash	
	Mangaoni Lapilli Formation (5 members)	
Cross bedded ash		
Shower-bedded ash		
Flow units		
Shower-bedded ash	Rotoehu Ash	Rotoiti Breccia Formation
Flow units		
Shower-bedded ash		
Brown Ashes		
Ignimbrite	Mamaku Ignimbrite	

CHAPTER III

METHOD

In the course of the fieldwork from which this study is derived, Clifford collected over 200 samples of ash flow deposits at various localities within the Rotoiti Breccia Formation, North Island, New Zealand. At each locality, the maximum pumice and lithic clast sizes were determined and features such as the presence of absence of layering and grading were noted. Zones of pumice or lithic concentrations were also noted.

In this study, 18 samples from proximal, medial, and distal areas of the flow were examined. A chart showing which area each sample is from is included (see fig.2). The proximal samples were collected from a zone 5 to 10 km. from the source area while the distal samples were collected from the most outlying areas of the flow, near the Bay of Plenty. The medial samples were collected from areas between these two zones. The sample locations are noted on the map of the Rotoiti Breccia (fig. 2).

The samples were sieved with a set of sieves having an interval of one phi unit, and covering a range of sizes from -4Ø (16 mm.) to 4Ø (1/16 mm.). The sieving was done by hand to reduce to a minimum the amount of pumice abrasion that would result from the use of a standard mechanical shaker (see Walker, 1971). Even so, some unavoidable abrasion did occur producing an excess of fine particles which introduces some error into the measurements. The results of this analysis were plotted as cumulative frequency curves on arthimetic probability paper (fig. 3-20) and the median grain diameter (MdØ) and the graphic standard deviation (Ø) or sorting were determined. The Inman parameters MdØ $(=\phi_{50})$ and $\sigma\phi$ $(= \phi_{84}-\phi_{16}\ /2)$ were used. The validity of this particular method of statistical analysis is based on the assumption that the grain size distribution of any sample is approximately log-normal. There has been some argument in the literature that a grain size distribution resulting from an explosive eruption is better described by Rosin's Law of Crushing (Kittleman, 1964). Sheridan (1971) feels that it is uncertain as to which law better describes such a distribution, but the statistical parameters of normal curves are easier to work with and using them facilitates comparison to other examples in the literature (esp. Walker, 1971).

The eighteen samples were further analyzed by separating each size grade down to ½ mm. into the three main components of pyroclastic rocks; pumice, lithics, and crystals. The pumice category includes pumice, glass shards derived from pumice, and dense glassy rock fragments representing non-vesiculated magma. Lithics include any material within the flow not directly derived from the magma such as vent wall rock fragments or particles incorporated into the flow from the ground and are usually recognized by their darker colour and higher density. The crystals were differentiated from glass fragments by the presence of one or more cleavage faces and by their crystal form. The crystal mineralogy and petrology is given in Chapter VI. The results of this analysis were plotted as triangular diagrams and as histograms showing the relative proportions of pumice, lithics, and crystals.

While separating out the components under a binocular microscope, the shape and degree of roundness of pumice shards were examined for samples from both proximal and distal areas.

To determine the original crystallinity of the magma, a few of the largest pumice fragments were crushed until all of the resulting fragments passed through the -2Ø sieve--a size comparable to the largest crystals. The crushed pumice was then sieved and crystals were removed from each size grade. Their weight percent was determined allowing calculation of the original bulk crystallinity of the magma.

TABLE 2

SAMPLES

PROXIMAL	MEDIAL	DISTAL
R-086	R-061	R-022
R-088	R-089	R-040
R-129	R-093	R-139
R-131	R-144	R-143
R-132	R-145	
R-193	R-150	
R-194		
R-197		

CHAPTER IV

RESULTS

The results of the grain size analyses are given as cumulative frequency curves in figures 3 to 20. The dominant features of all of these curves is the poor degree of sorting displayed and the lack of any significant differences in sorting between proximal and distal areas. To examine these further, the median grain diameter and sorting values were determined for each sample in the manner outlined above and plotted on an Mdϕ vs $\sigma\phi$ graph (figure 21). The sorting values range from 2ϕ to 4ϕ and the median diameter values range from 0.25ϕ to 2.25ϕ. These values fall approximately in the middle flow field of an Mdϕ,$\sigma\phi$ plot as determined by Walker (1971), confirming that these deposits are in fact derived from a pyroclastic flow. The samples from the proximal, medial, and distal areas are differentiated in the plot showing that there is no specific grouping of values unique to any of these areas present in the flow. Rather, there is a fairly wide variation within any one particular flow area.

The significant difference between the proximal and the distal areas is in the nature of the grain size populations themselves. The medial and distal curves are essentially unimodal (with minor deviations) as only one straight line segment may be fitted to these curves. In one or two cases, there may be a hint of a bimodal population (e.g. R-139), but this is not pronounced and is, therefore, disregarded. The proximal curves, however, are distinctly bimodal as two straight line segments may be fitted to most of the curves. The best example of this is seen in sample R-131. Thus, two log-normal populations are present in the proximal areas.

The results of the component analyses are given as triangular plots (figs. 22 to 30) and histograms (figs. 31 to 34), both of which show the proportions of pumice, lithics, and crystals relative to the total for each grain size. While the histograms give a better idea of the contribution of each component at a particular grain size, the triangular plots better show the trends of each component as the grain size decreases.

In all of the plots, the general trend is for pumice to be dominant at the largest grain sizes (16 mm.), and for the lithics to be much less important. Crystals do not appear until smaller (1 mm.) grain sizes. As the grain size decreases, the lithic population increases in importance to a maximum of roughly 40 weight %. This occurs at about 4 to 8 mm. A further decrease in grain size sees the lithics steadily decline in importance. At 2 mm. and 1 mm., crystals appear and very rapidly become the dominant component at the finer grain sizes.

The bulk crystallinity of the crushed pumice sample and hence of the original population was determined to be approximately 15% by weight. This corresponds to a 6.5:1 ratio of pumice to crystals. Compared to this ratio, all of the Rotoiti Breccia samples show a marked increase in crystal content; however, there are some significant variations between the samples of different areas. When the ratios of pumice to crystals are compared to the original bulk ratio, it is found that the crystal enrichment factor in distal and medial samples is on the order of 10X, and in some cases, may be as high as 20X. Proximal samples, on the other hand, only show a crystal enrichment factor on the order of 2X. This trend shows up very well on the triangular diagrams. Typical triangular plots for proximal samples show a fairly tight grouping of points near the pumice apex of the diagram. Crystals are becoming more prevalent at 1 and ½ mm. sizes, but only to approximately 15 weight % (of combined pumice, lithics, and crystals). Pumice is still the major component at all grain sizes. The plots for medial/distal samples show a much more distinct trend towards the crystal apex of the plot with decreasing grain size. Thus, crystals are becoming the major component on the order of 60 to 70 weight % at the finer grain sizes.

The pumice samples from proximal areas examined at random showed a much lower degree of rounding and sphericity than pumice samples from distal areas. The axes of proximal pumice grains had relative dimensions of approximately 3:1:1 while the axes of distal pumice grains approximated 1.5:1:1. The controlling factor of the long axis of the pumice grains is the direction in which the gas vesicles are drawn out. Thus, distal pumices had a higher degree of sphericity. Also, the distal pumice grains had fairly smooth surfaces and could be classed as sub-rounded to rounded. The proximal pumice grains had shards still projecting out and, therefore, could only be classed as sub-angular to sub-rounded.

Figures 3 to 6. Cumulate Frequency Curves showing size distributions of samples from distal areas.

R 022

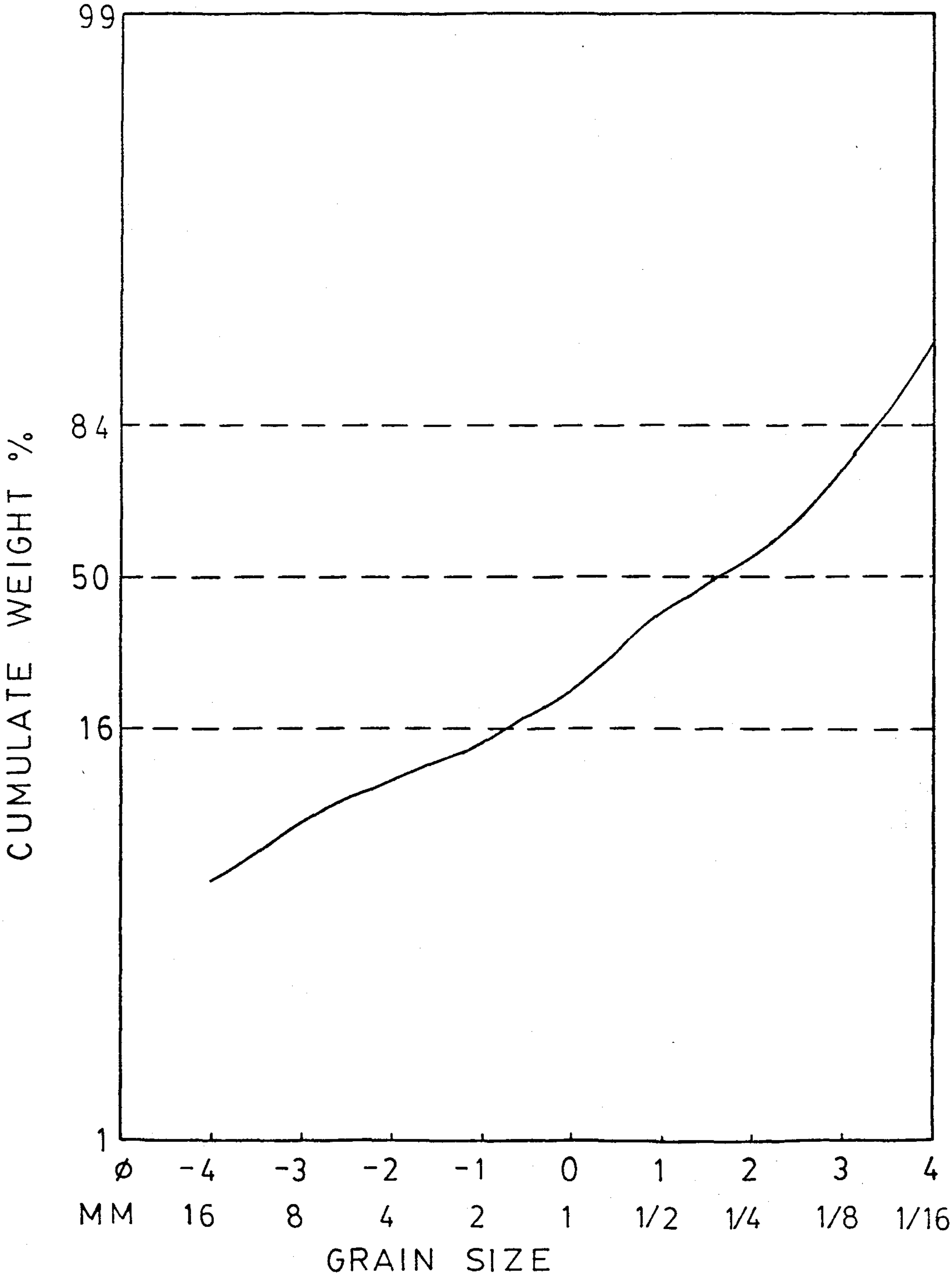
99
84
50
16
1
CUMULATE WEIGHT %
ϕ -4 -3 -2 -1 0 1 2 3 4
MM 16 8 4 2 1 1/2 1/4 1/8 1/16
GRAIN SIZE

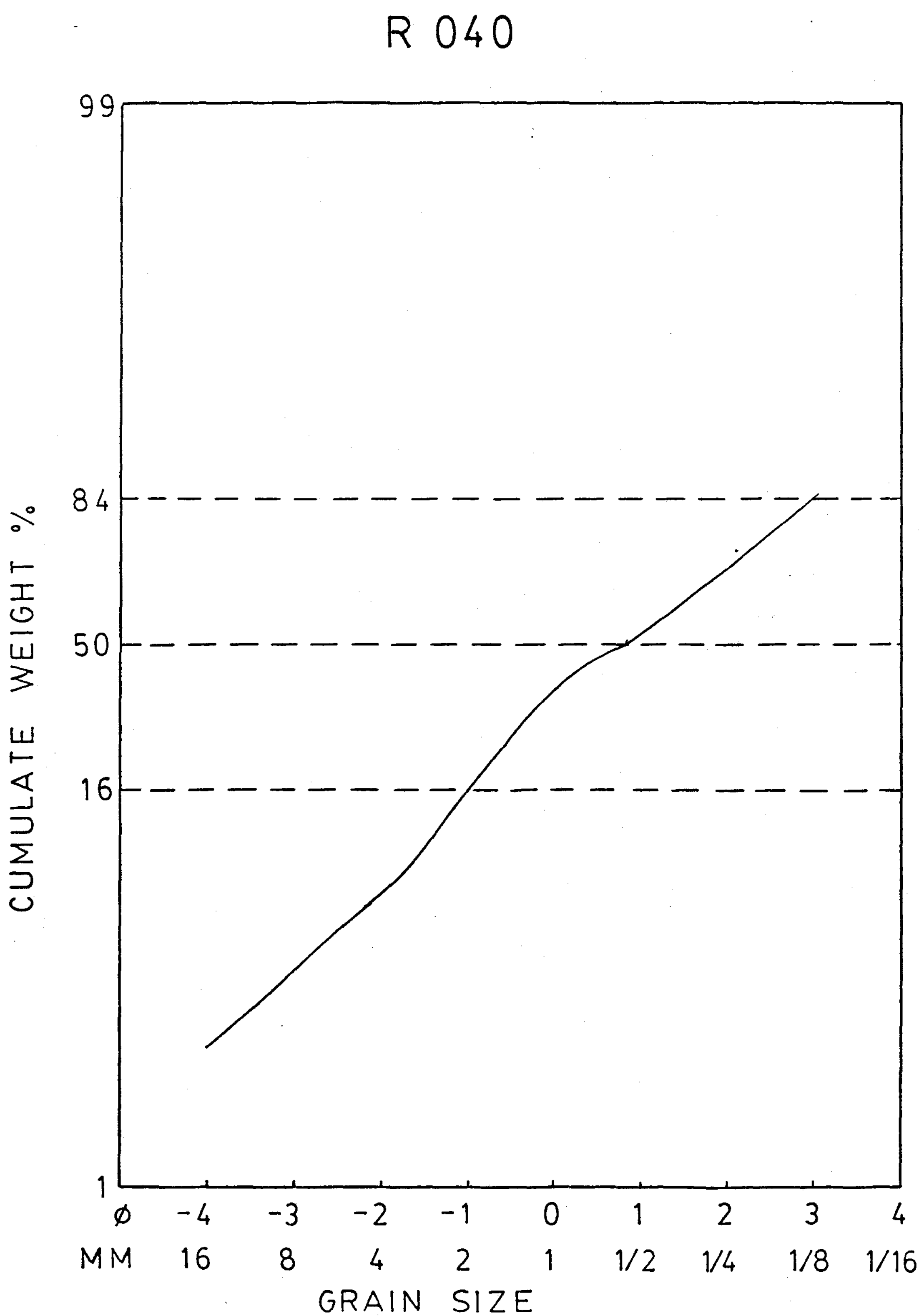
R 040
99
84
50
16
1
CUMULATE WEIGHT %
ø -4 -3 -2 -1 0 1 2 3 4
MM 16 8 4 2 1 1/2 1/4 1/8 1/16
GRAIN SIZE

R 139

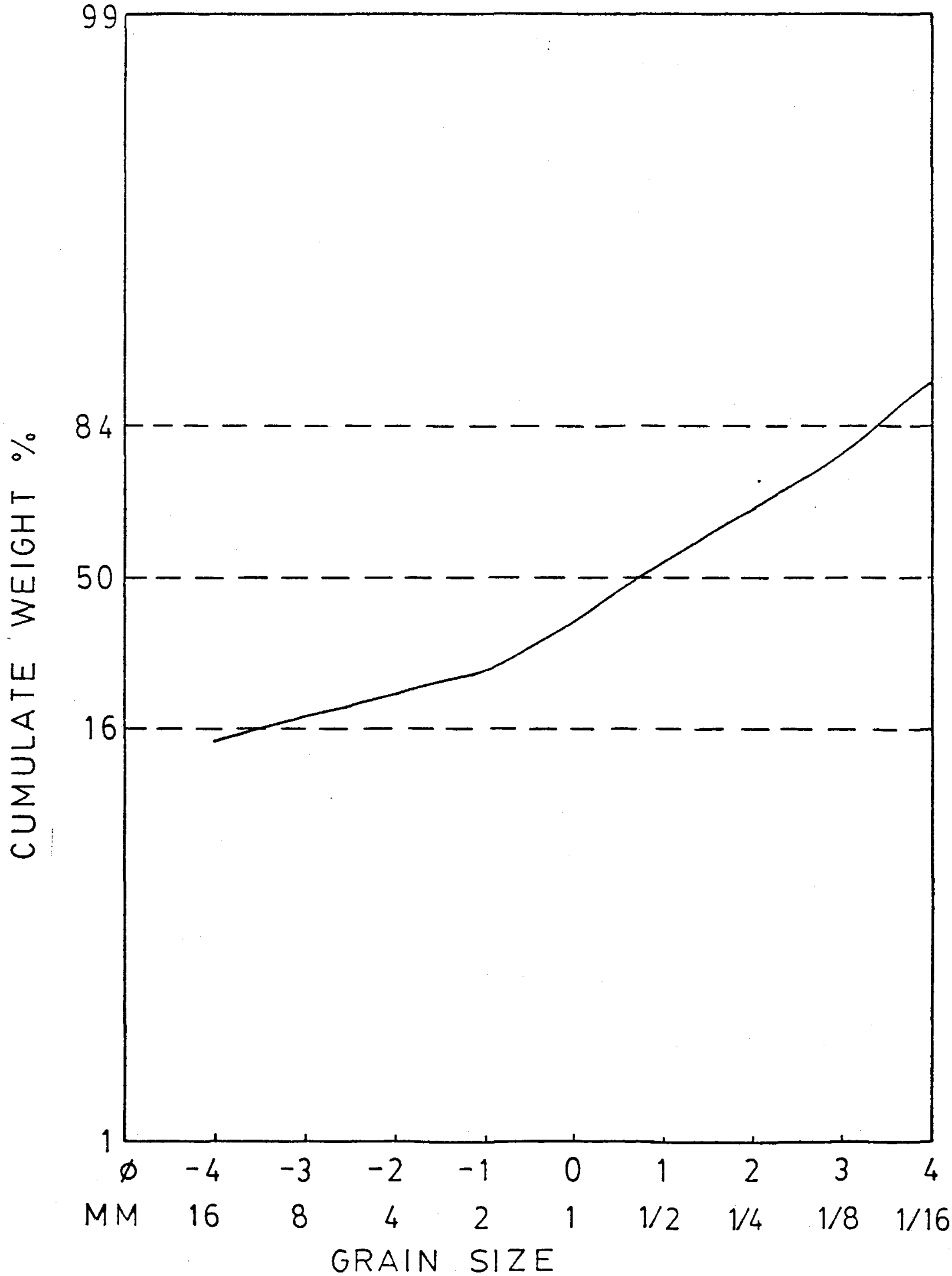
99
84
50
16
1
CUMULATE WEIGHT %
ø -4 -3 -2 -1 0 1 2 3 4
MM 16 8 4 2 1 1/2 1/4 1/8 1/16
GRAIN SIZE

R 143

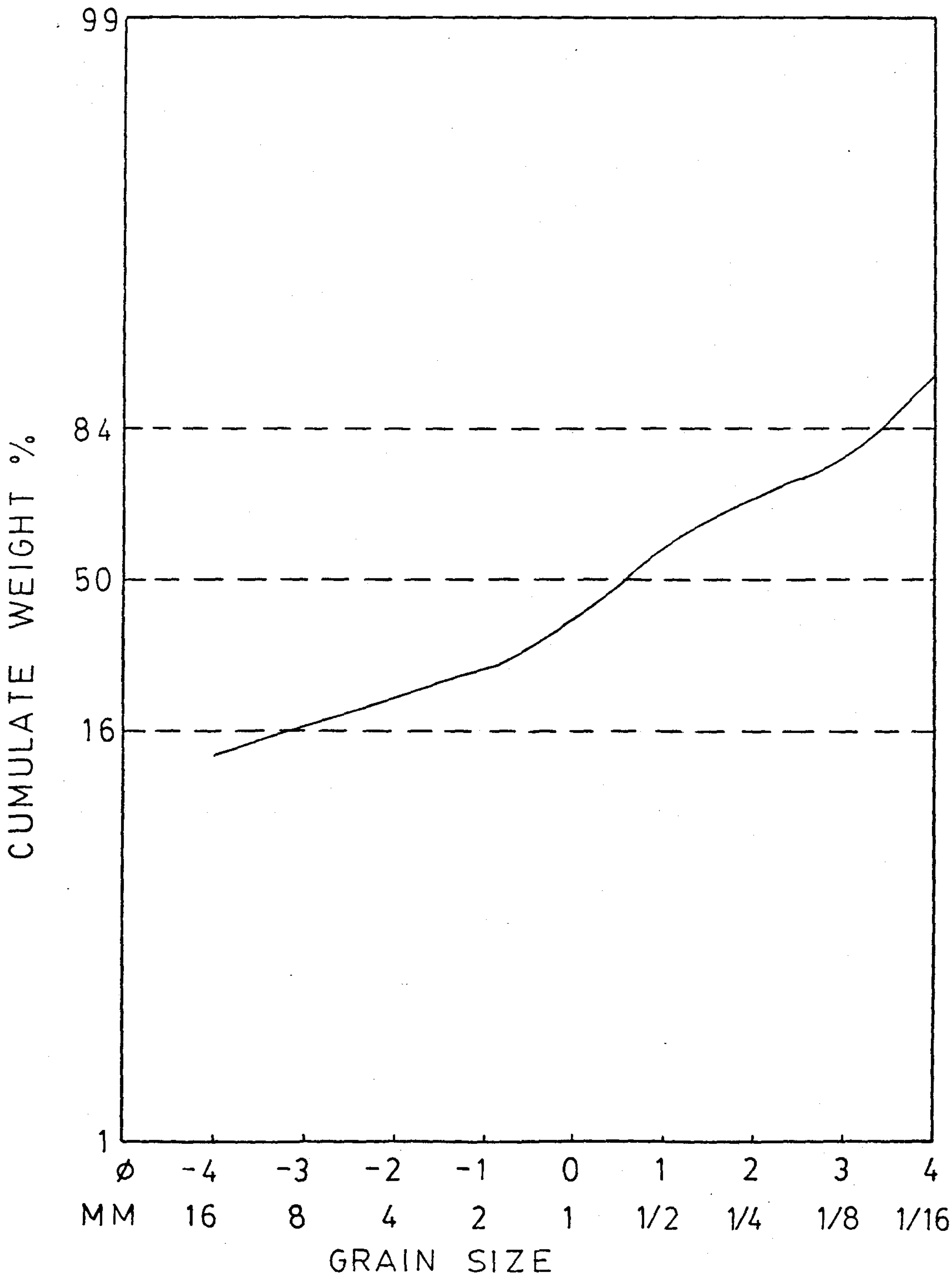
99
84
50
16
1
CUMULATE WEIGHT %
ø -4 -3 -2 -1 0 1 2 3 4
MM 16 8 4 2 1 1/2 1/4 1/8 1/16
GRAIN SIZE

Figures 7 to 12. Cumulate frequency curves showing size distributions of samples from medial areas.

R 061

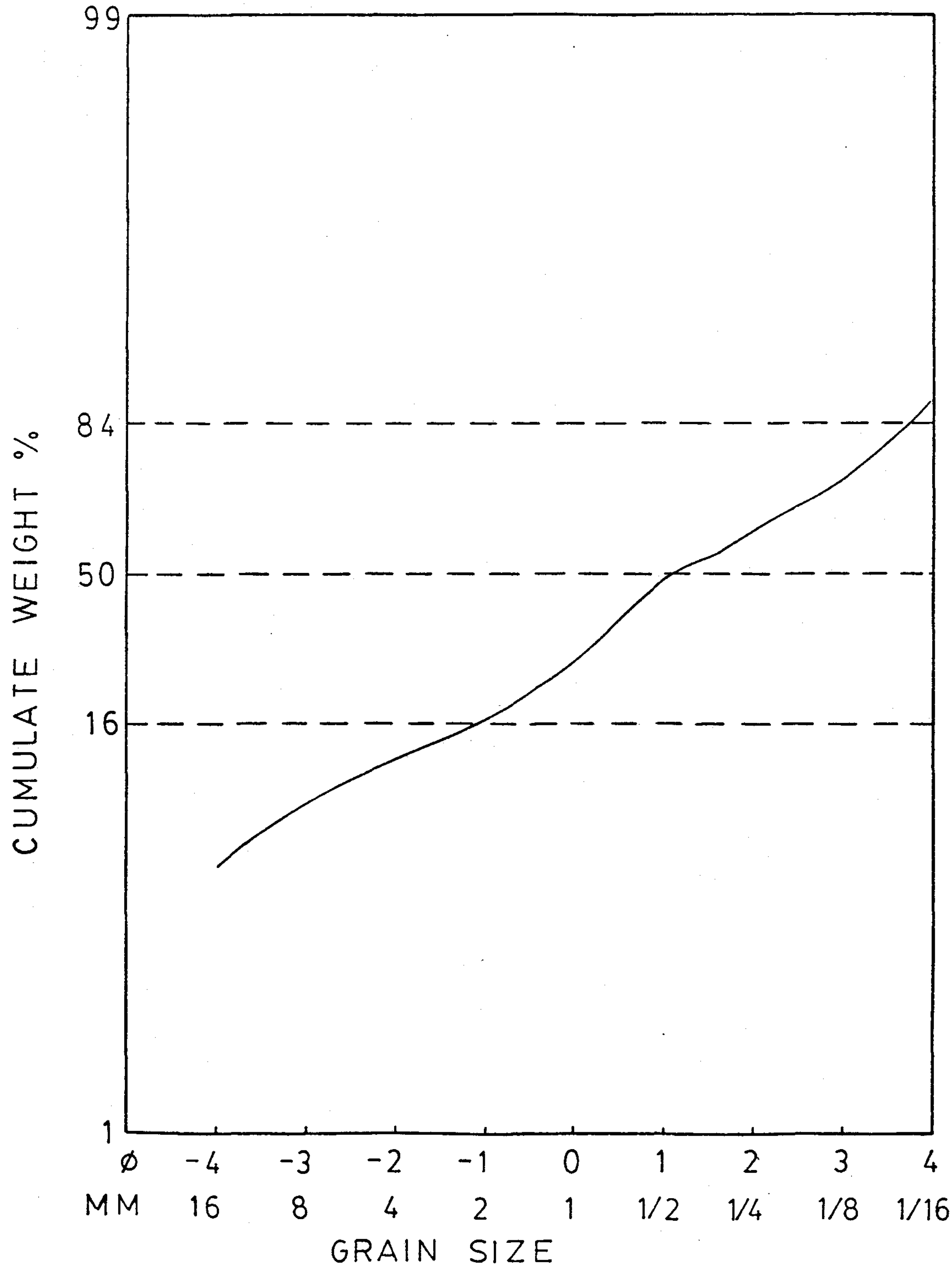
99
84
50
16
1
CUMULATE WEIGHT %
Ø -4 -3 -2 -1 0 1 2 3 4
MM 16 8 4 2 1 1/2 1/4 1/8 1/16
GRAIN SIZE

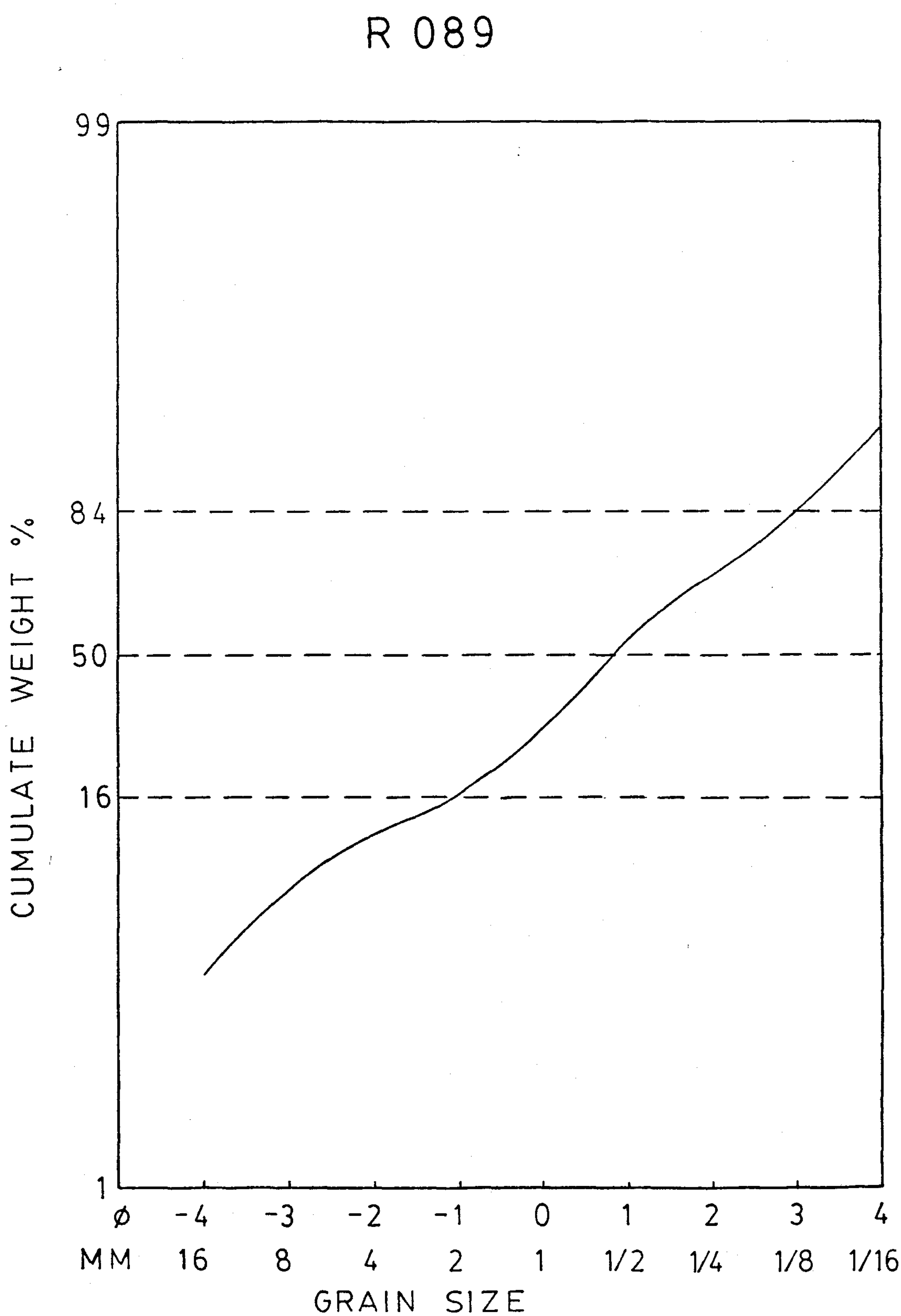
R 089
99
84
50
16
1
CUMULATE WEIGHT %
ø -4 -3 -2 -1 0 1 2 3 4
MM 16 8 4 2 1 1/2 1/4 1/8 1/16
GRAIN SIZE

R 093

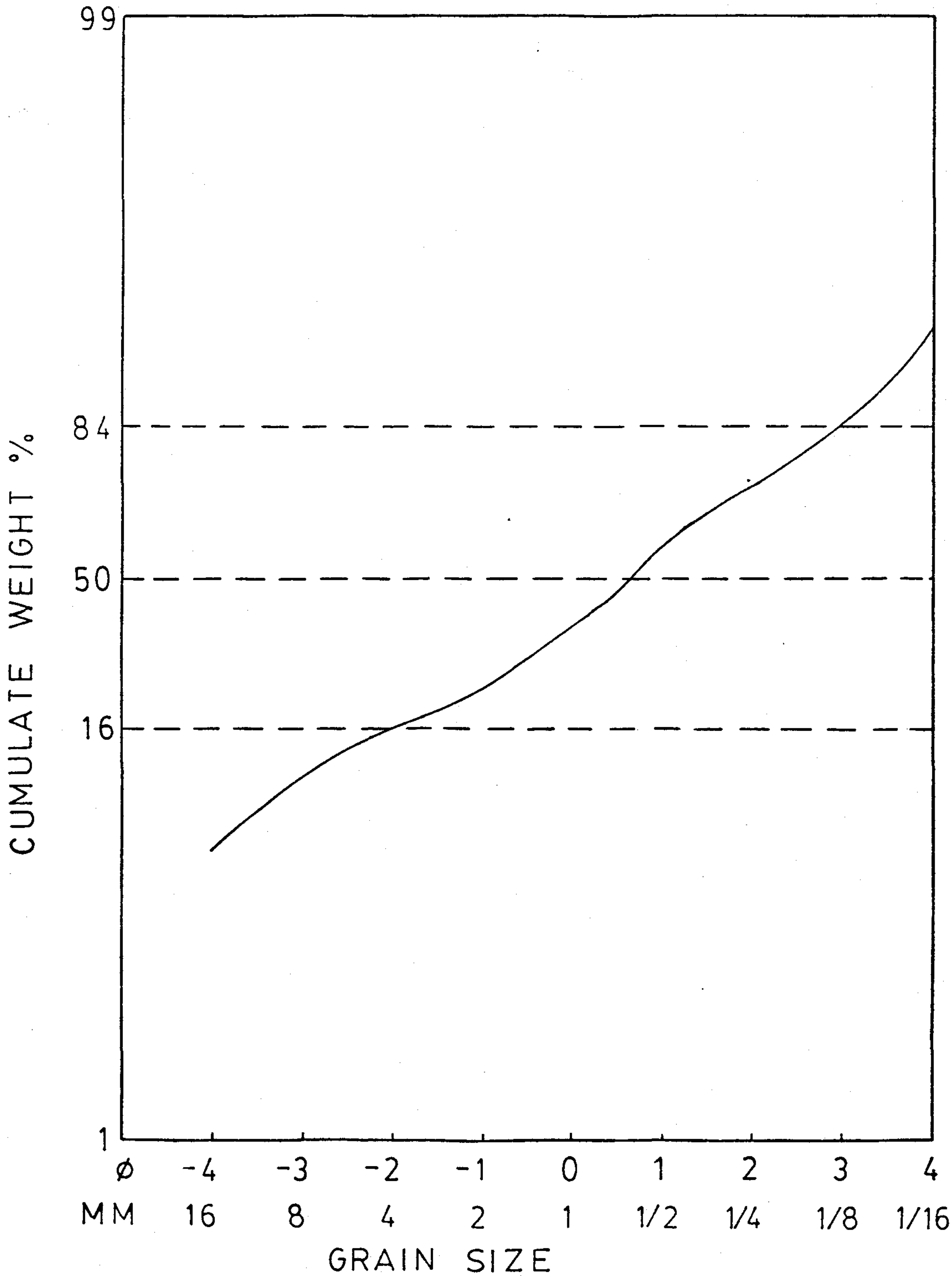
99
84
50
16
1
CUMULATE WEIGHT %
Ø -4 -3 -2 -1 0 1 2 3 4
MM 16 8 4 2 1 1/2 1/4 1/8 1/16
GRAIN SIZE

R 144

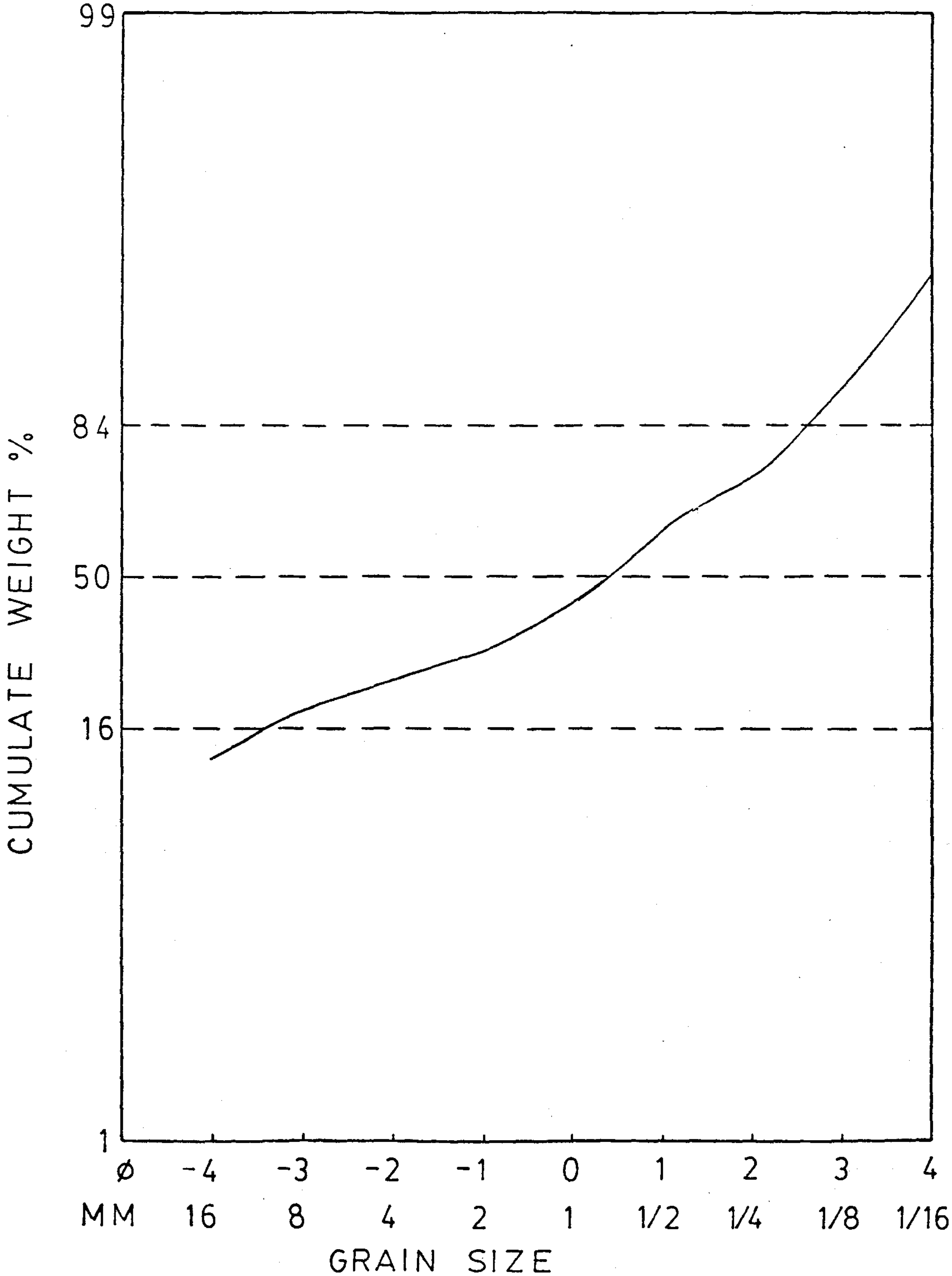
99
84
50
16
1
CUMULATE WEIGHT %
Ø -4 -3 -2 -1 0 1 2 3 4
MM 16 8 4 2 1 1/2 1/4 1/8 1/16
GRAIN SIZE

R 145

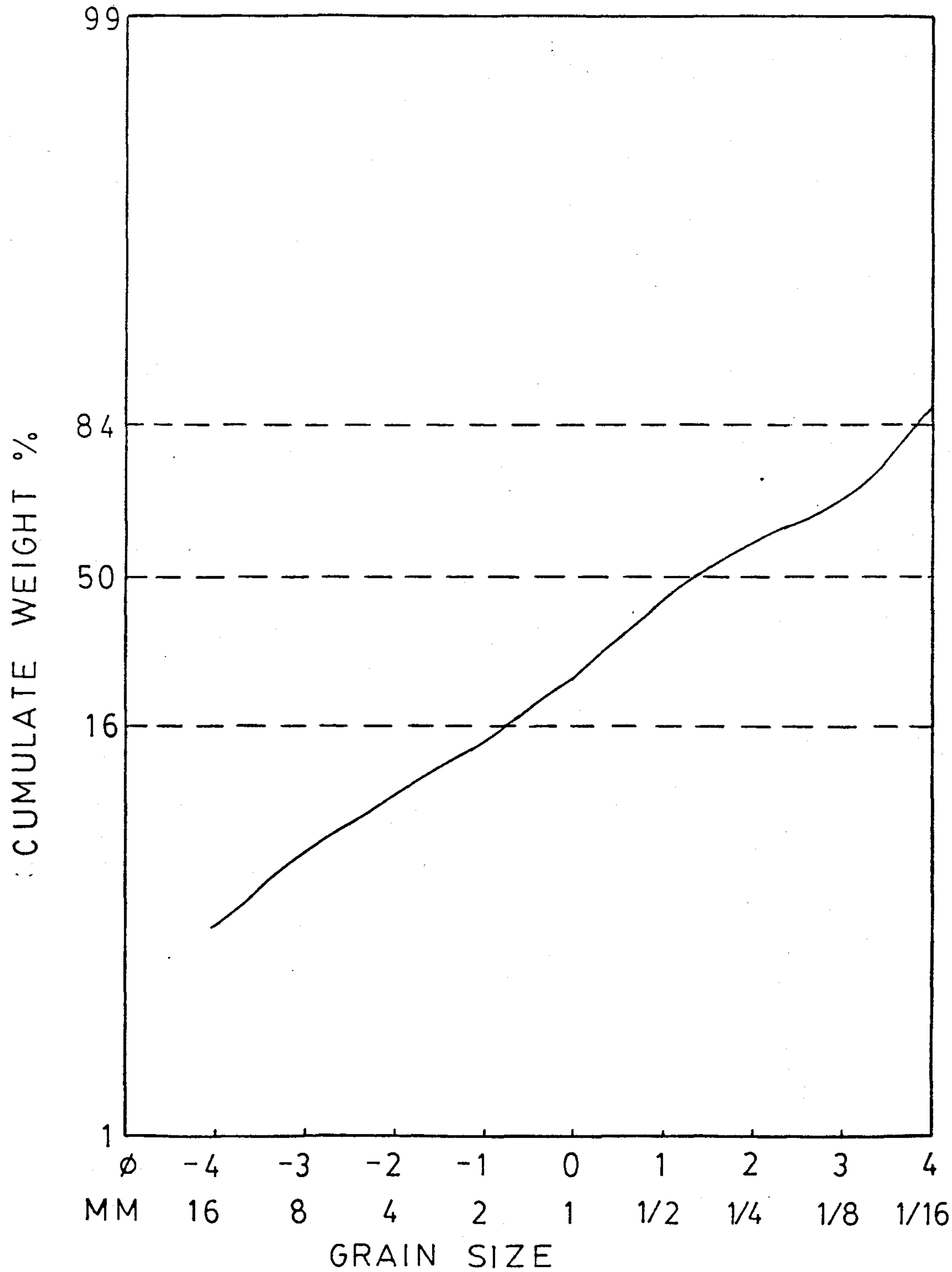
99
84
50
16
1
CUMULATE WEIGHT %
Ø -4 -3 -2 -1 0 1 2 3 4
MM 16 8 4 2 1 1/2 1/4 1/8 1/16
GRAIN SIZE

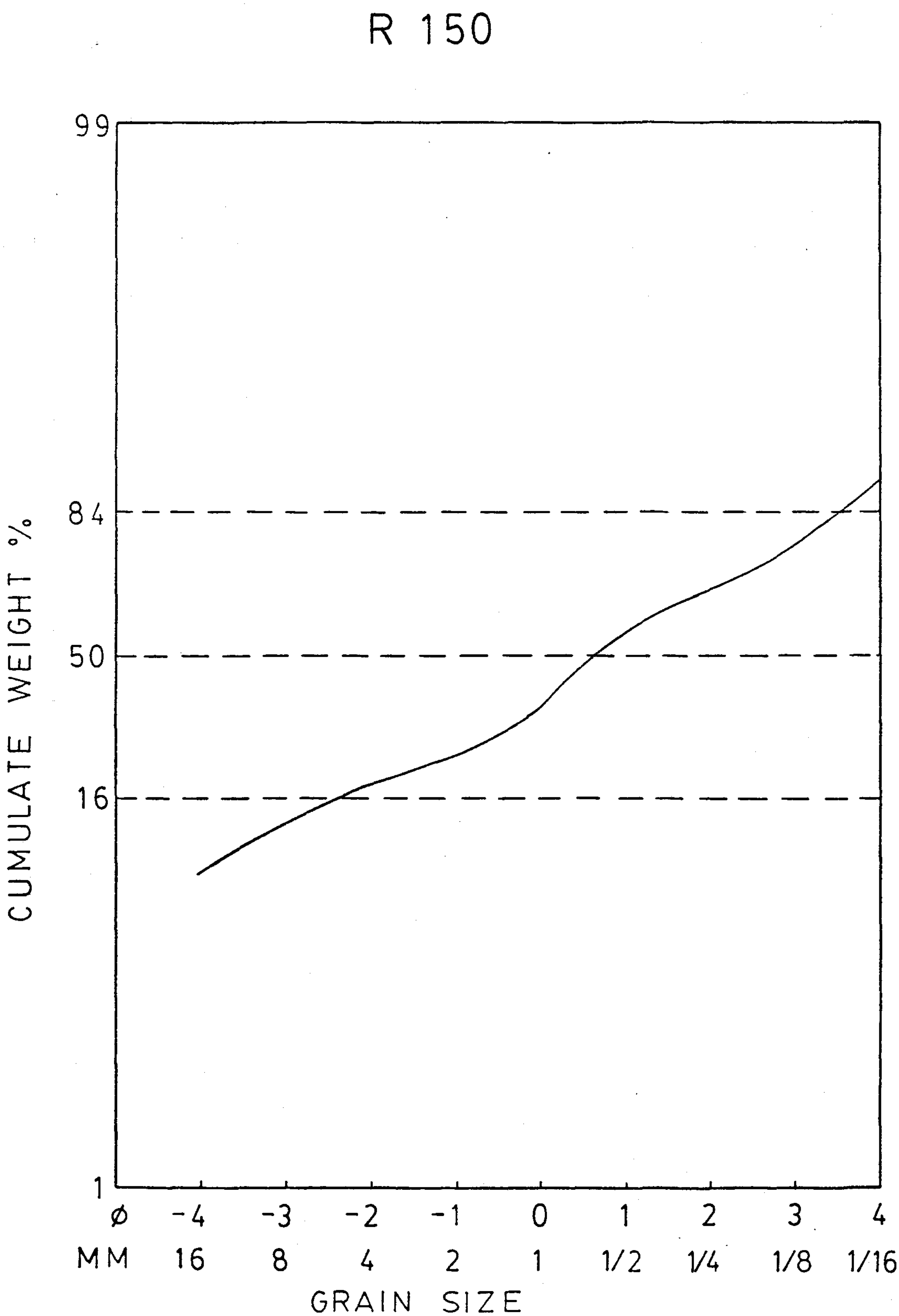
R 150
99
84
50
16
1
CUMULATE WEIGHT %
Ø -4 -3 -2 -1 0 1 2 3 4
MM 16 8 4 2 1 1/2 1/4 1/8 1/16
GRAIN SIZE

Figures 13 to 20. Cumulate frequency curves showing size distributions of samples from proximal areas.

R 086

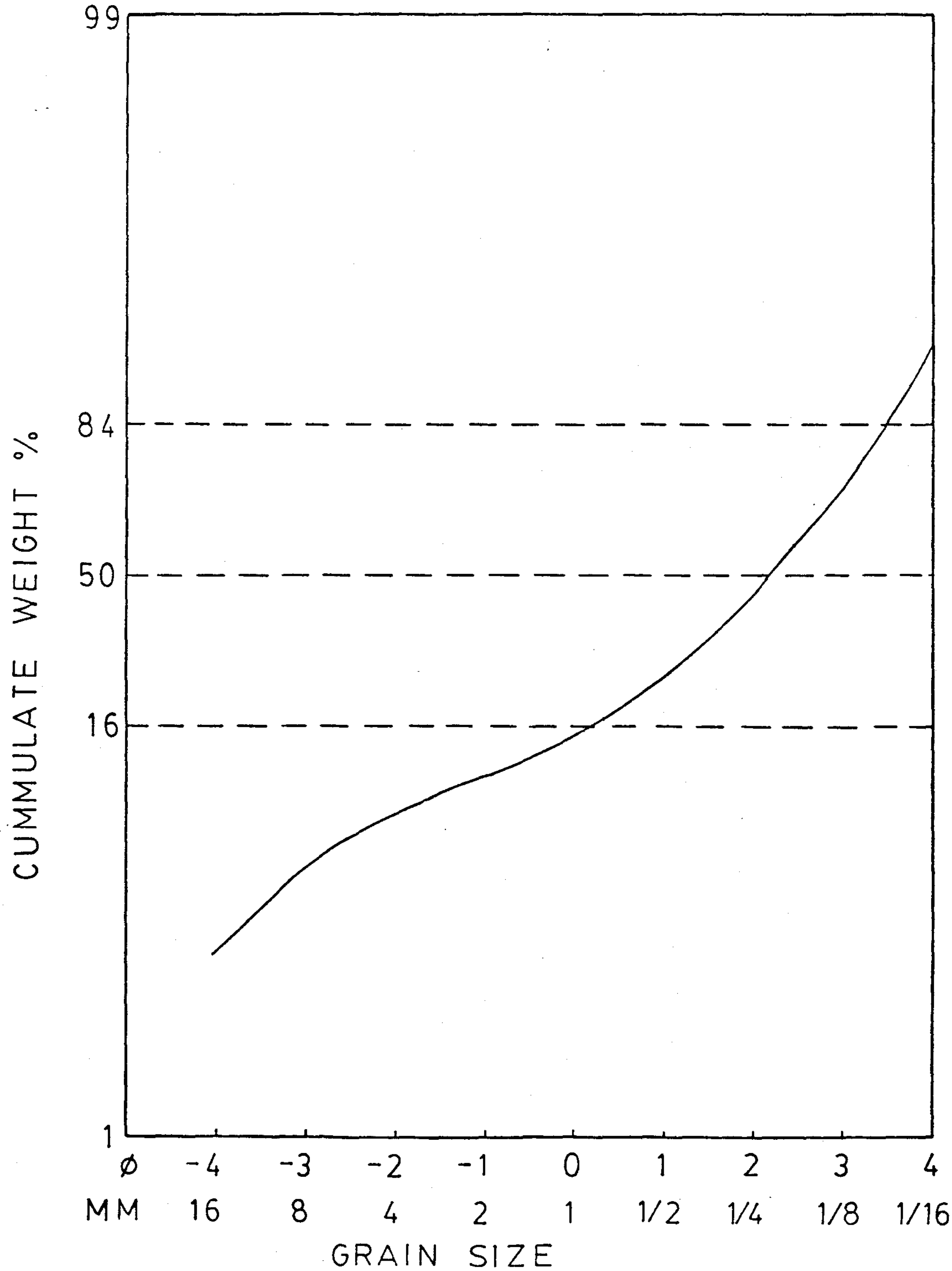

99
84
50
16
1
CUMMULATE WEIGHT %
ø -4 -3 -2 -1 0 1 2 3 4
MM 16 8 4 2 1 1/2 1/4 1/8 1/16
GRAIN SIZE

R 088

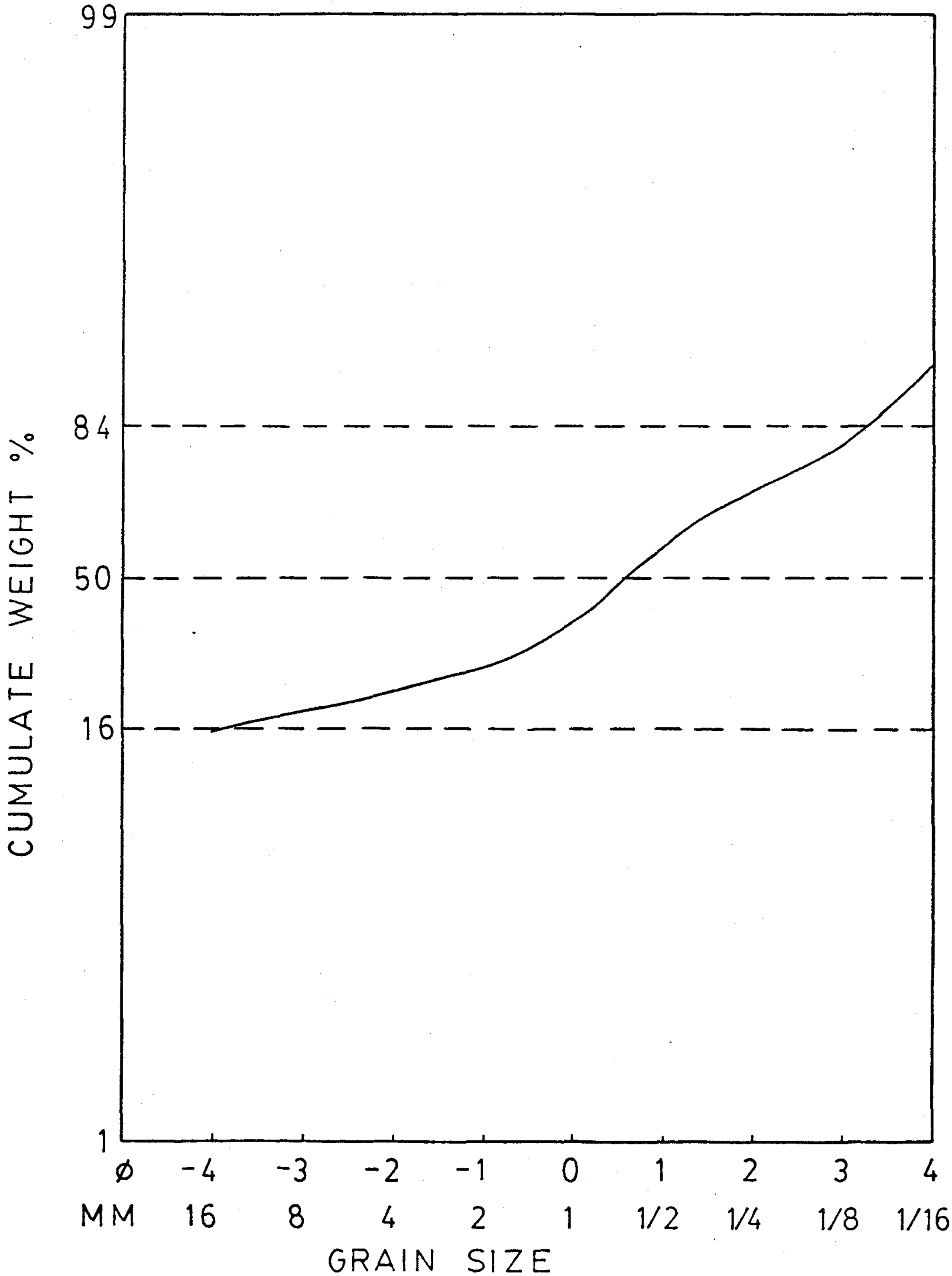
99
84
50
16
1
CUMULATE WEIGHT %
Ø -4 -3 -2 -1 0 1 2 3 4
MM 16 8 4 2 1 1/2 1/4 1/8 1/16
GRAIN SIZE

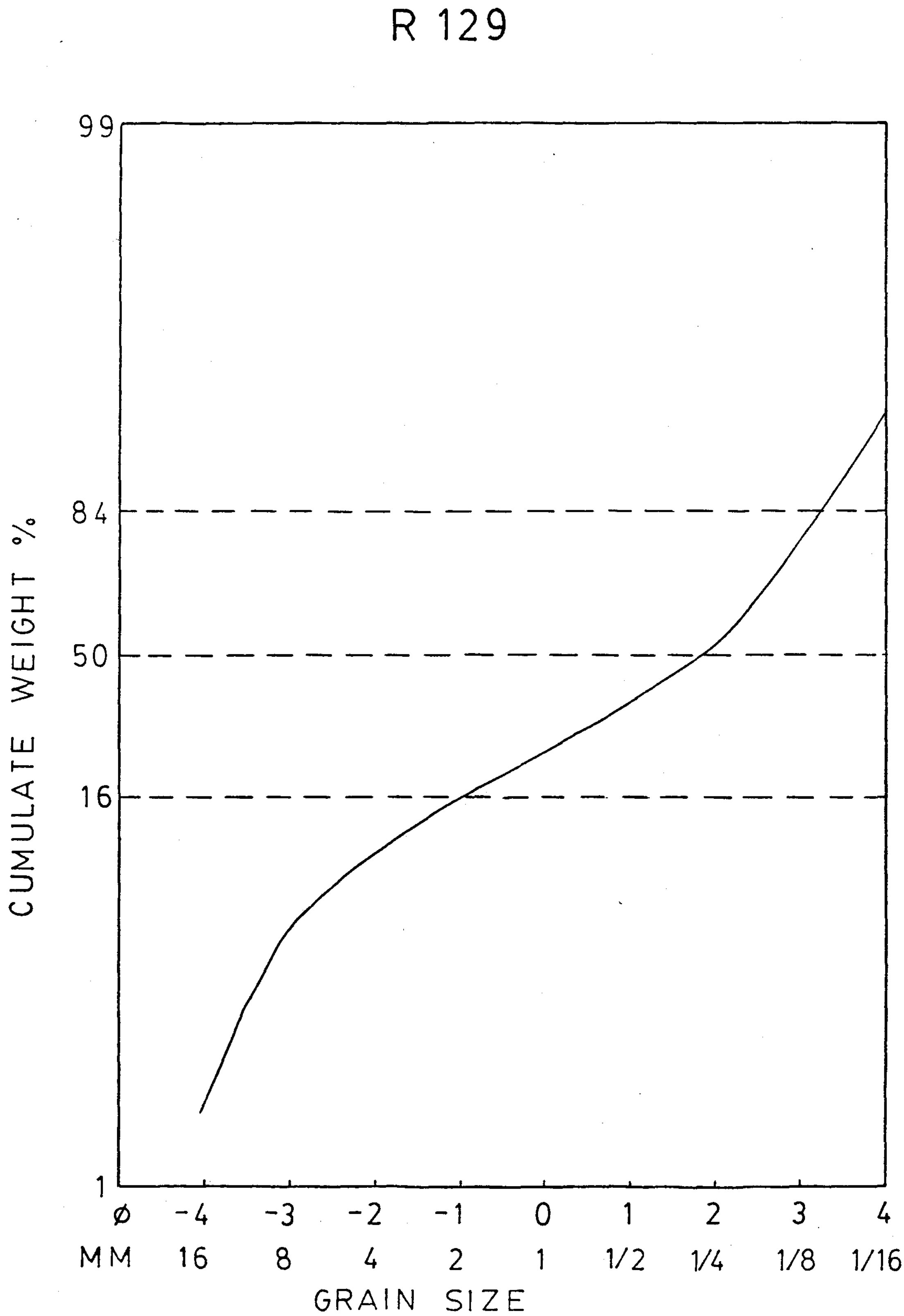
R 129
99
84
50
16
1
CUMULATE WEIGHT %
ø -4 -3 -2 -1 0 1 2 3 4
MM 16 8 4 2 1 1/2 1/4 1/8 1/16
GRAIN SIZE

R 131

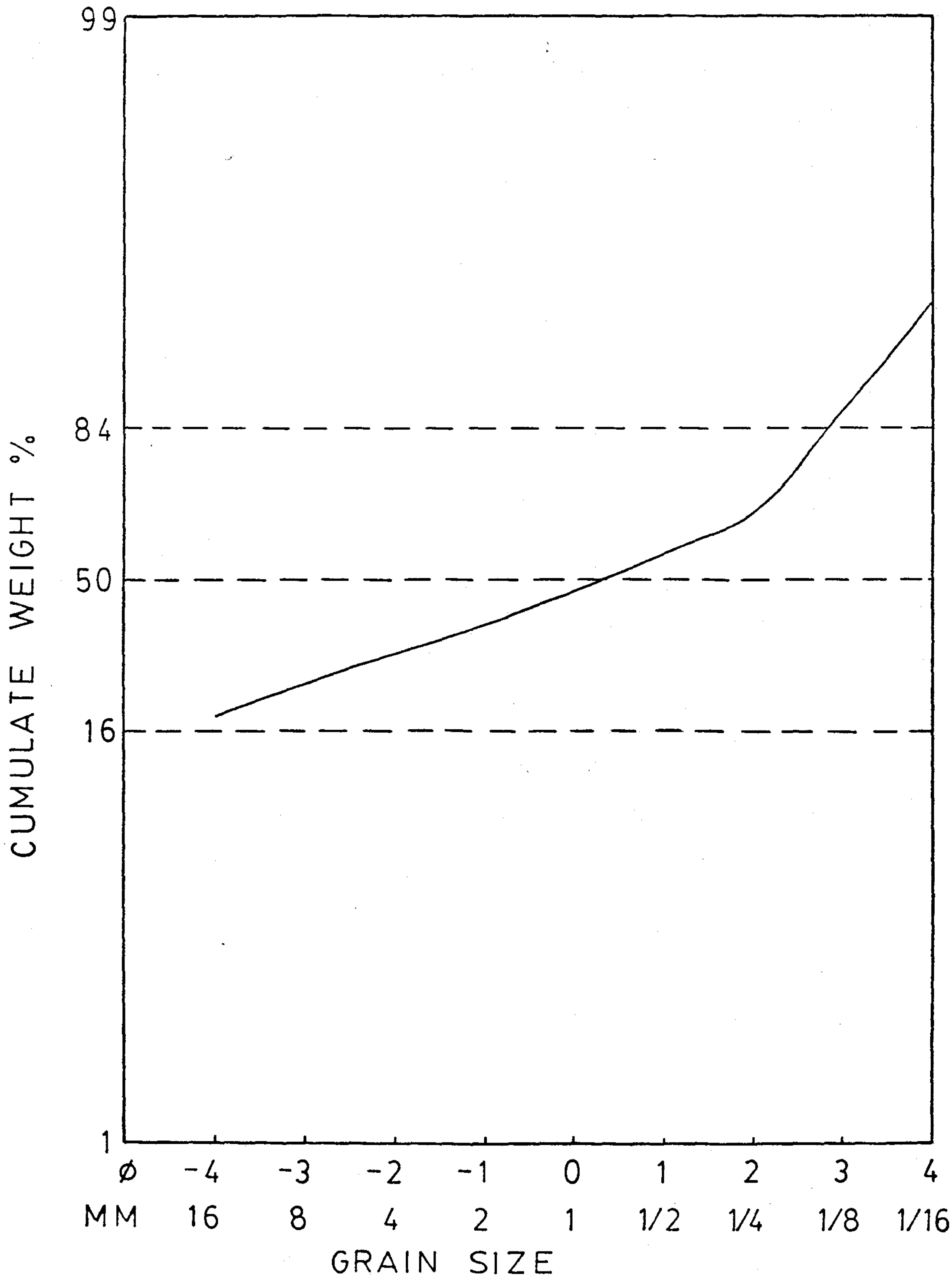

99
84
50
16
1
CUMULATE WEIGHT %
Ø -4 -3 -2 -1 0 1 2 3 4
MM 16 8 4 2 1 1/2 1/4 1/8 1/16
GRAIN SIZE

R 132

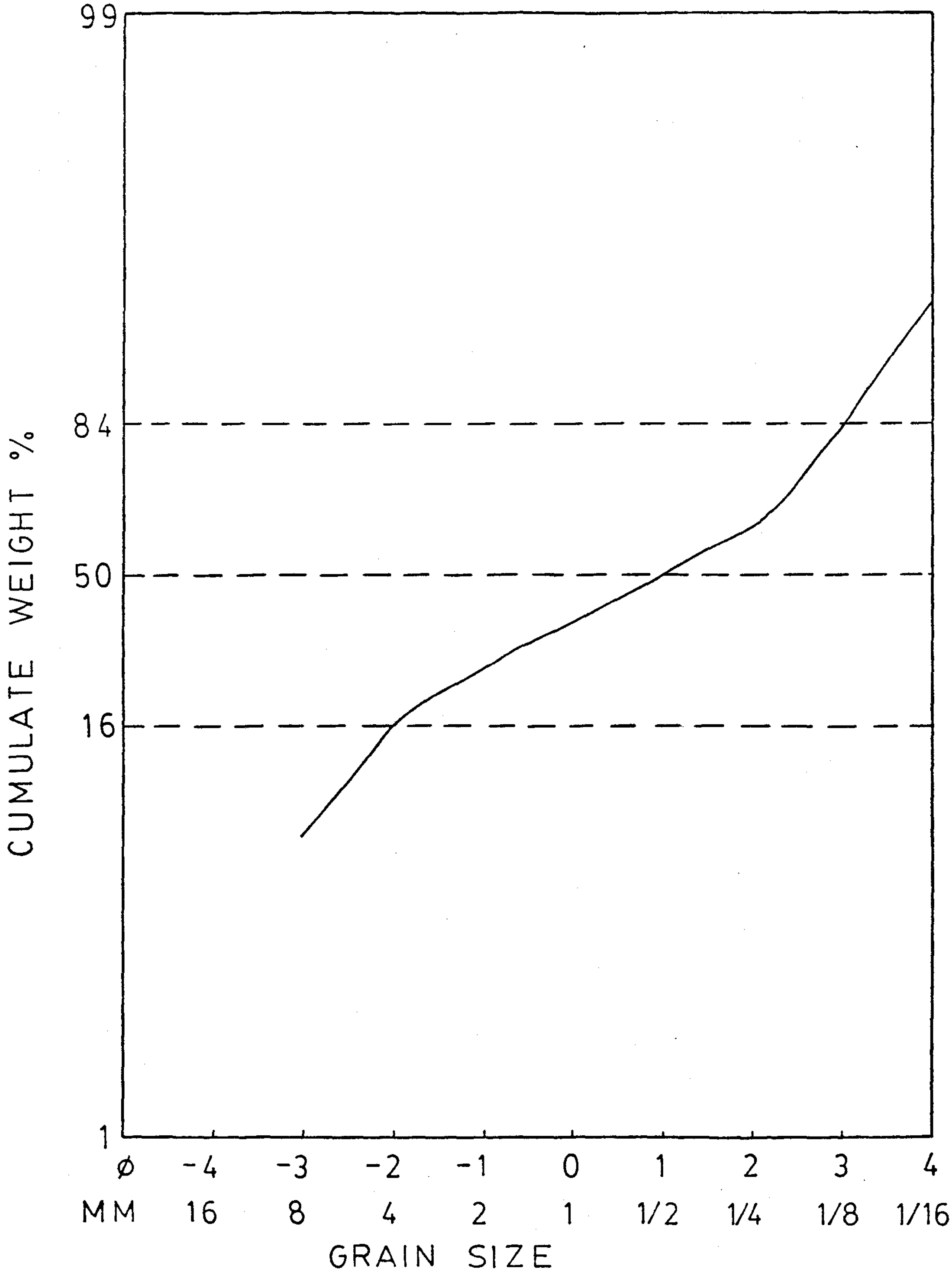
99
84
50
16
1
CUMULATE WEIGHT %
Ø -4 -3 -2 -1 0 1 2 3 4
MM 16 8 4 2 1 1/2 1/4 1/8 1/16
GRAIN SIZE

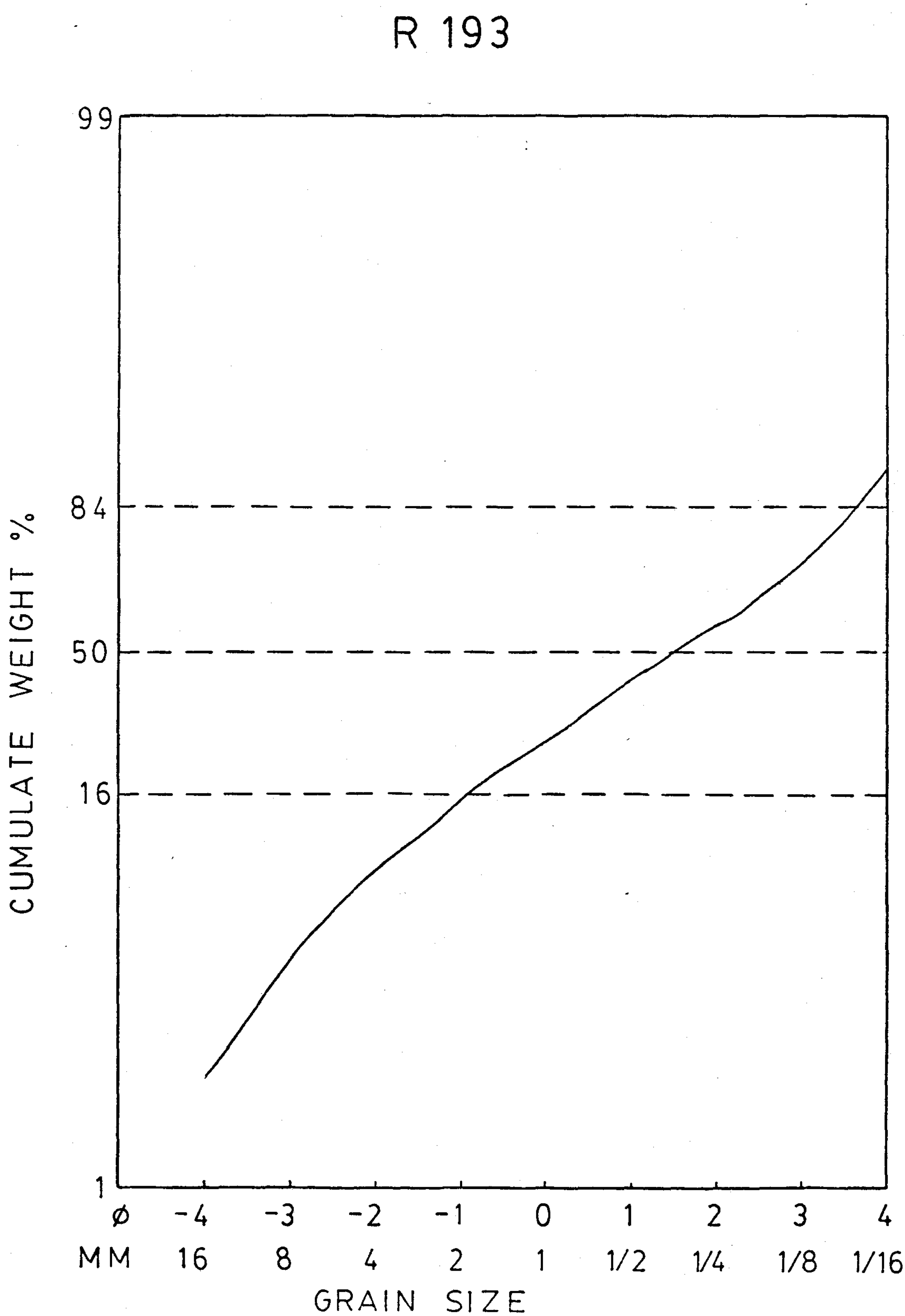
R 193
99
84
50
16
1
CUMULATE WEIGHT %
ø -4 -3 -2 -1 0 1 2 3 4
MM 16 8 4 2 1 1/2 1/4 1/8 1/16
GRAIN SIZE

R 194

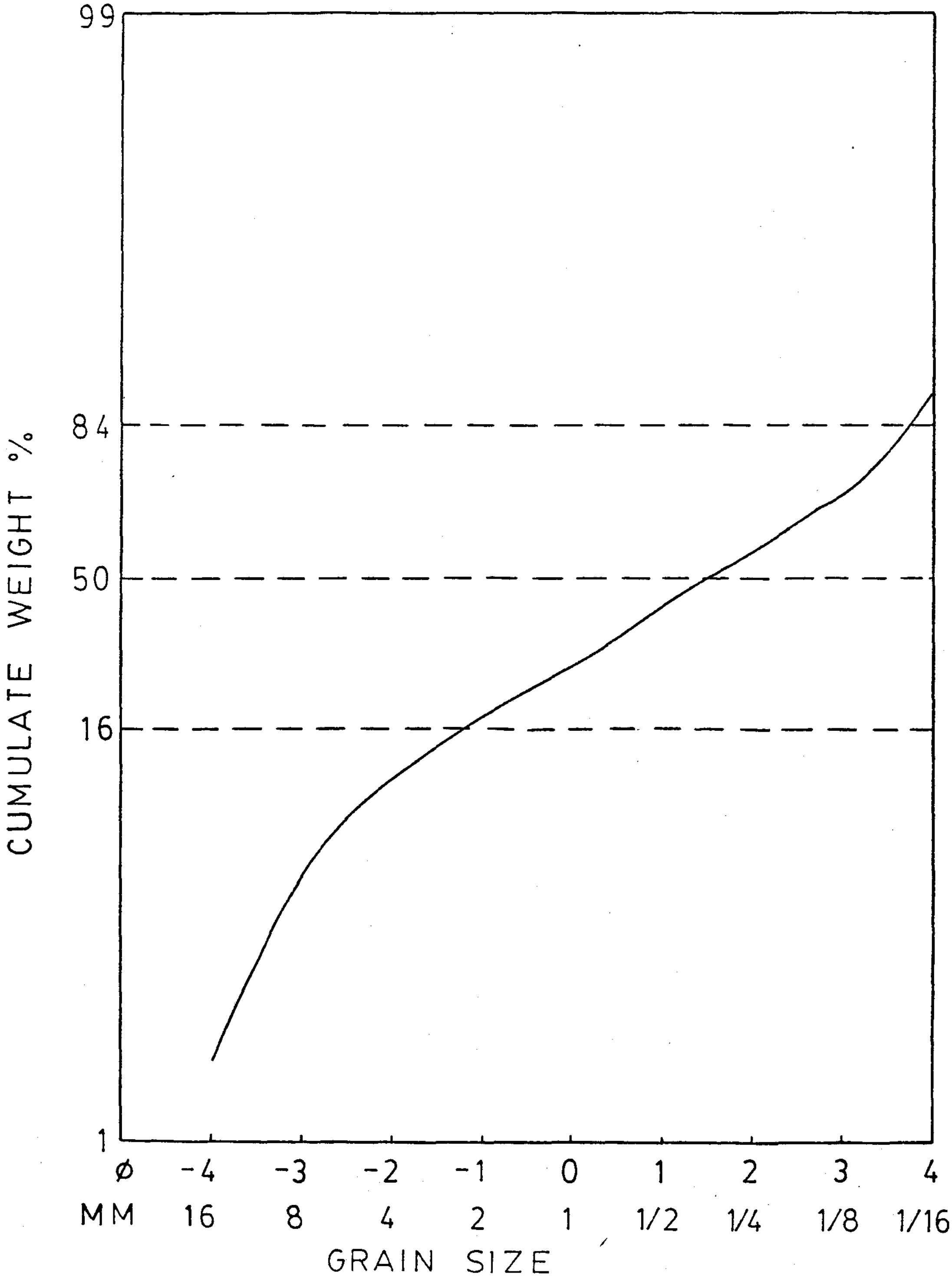
99
84
50
16
1
CUMULATE WEIGHT %
Ø -4 -3 -2 -1 0 1 2 3 4
MM 16 8 4 2 1 1/2 1/4 1/8 1/16
GRAIN SIZE

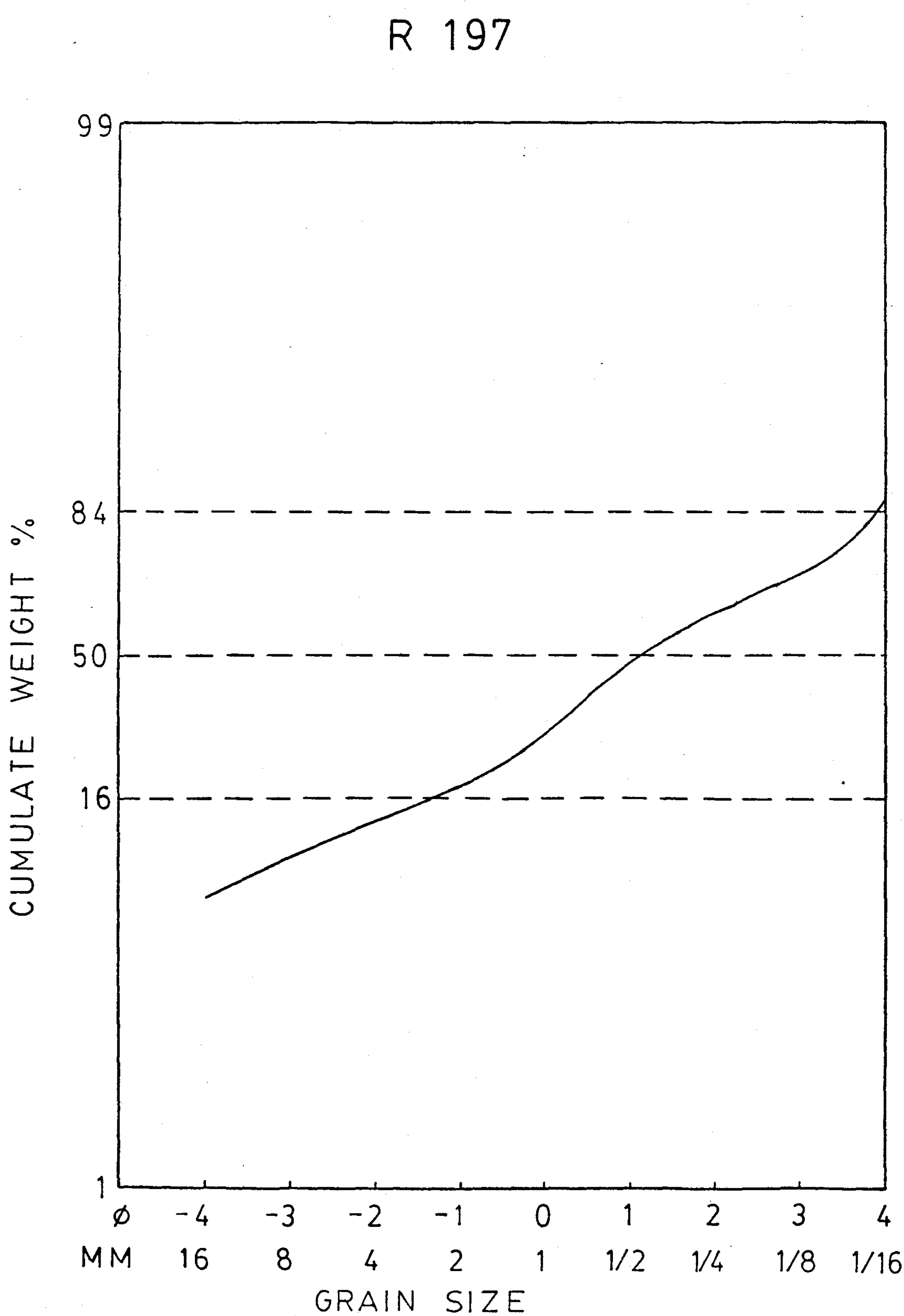
R 197
99
84
50
16
1
CUMULATE WEIGHT %
ϕ -4 -3 -2 -1 0 1 2 3 4
MM 16 8 4 2 1 1/2 1/4 1/8 1/16
GRAIN SIZE

Figure 21. Md∅ vs. ∅ plot for all samples. Distal samples denoted by +, medial samples denoted by x, proximal samples denoted by ⊙.

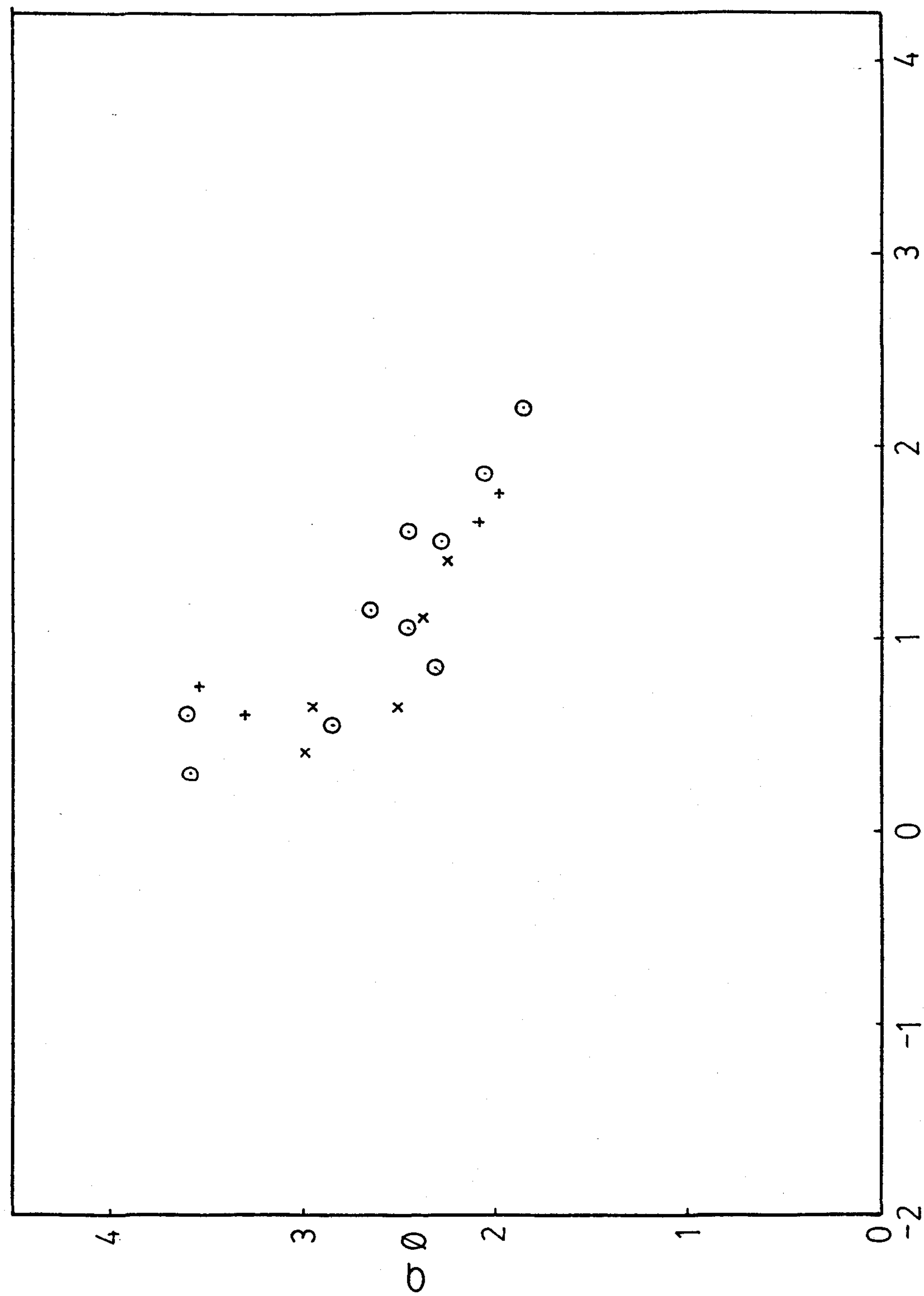

σØ
MdØ
0
1
2
3
4
-2
-1
0
1
2
3
4

Figures 22 to 23. Triangular diagrams for distal samples showing proportions of pumice (P), lithics (L), and crystals (C) at different grain sizes.

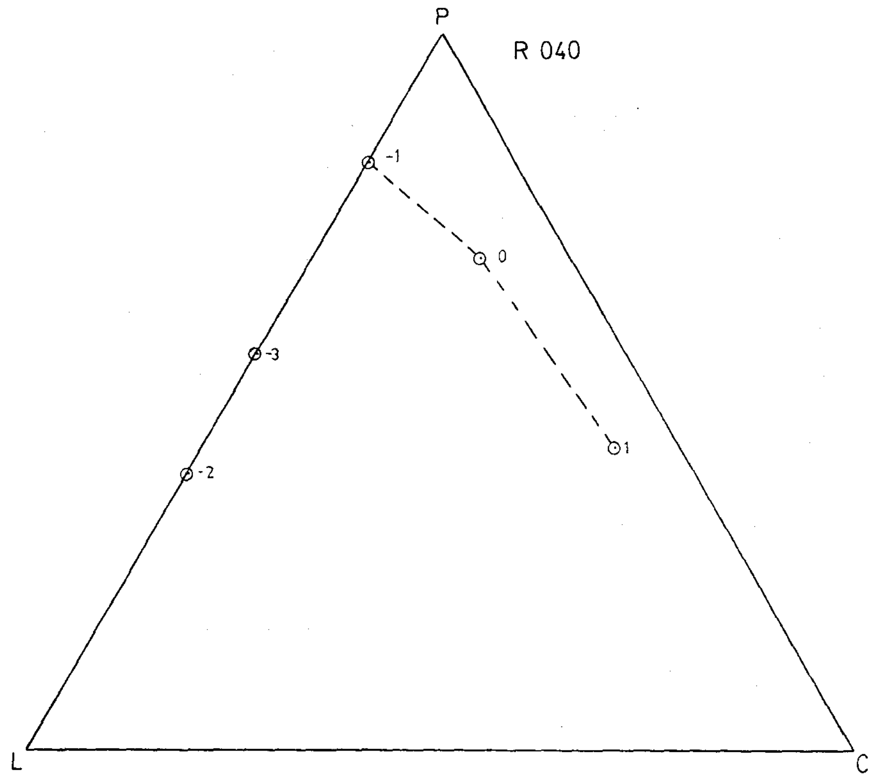
P
R 040
-1
0
-3
-2
1
L
C

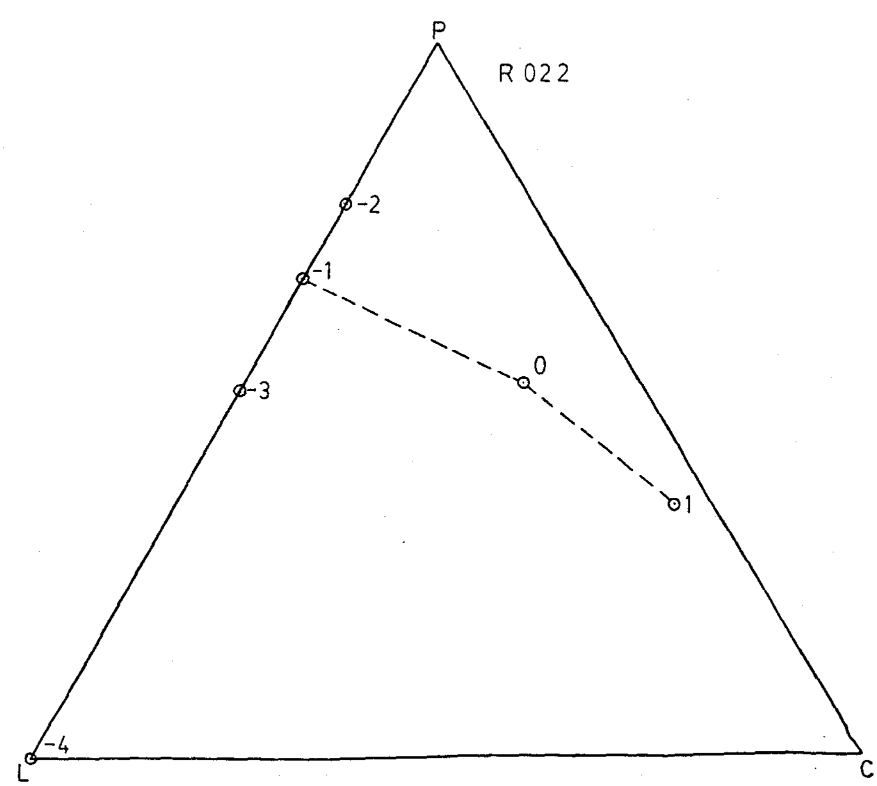
P
R 022
-2
-1
0
-3
1
-4
L
C

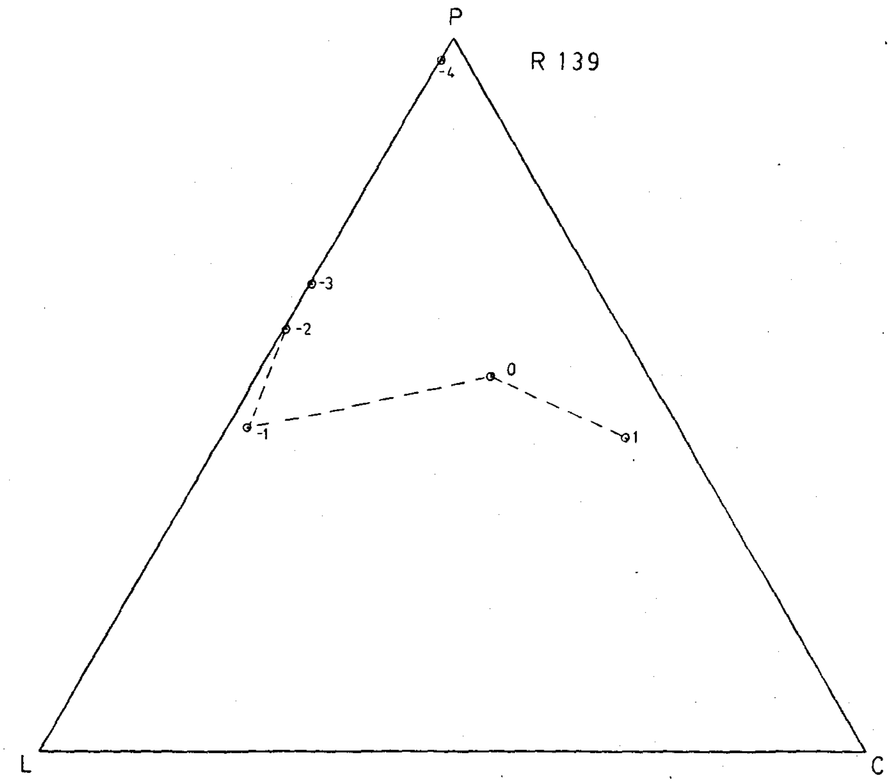
P
R 139
-4
-3
-2
0
-1
1
L
C

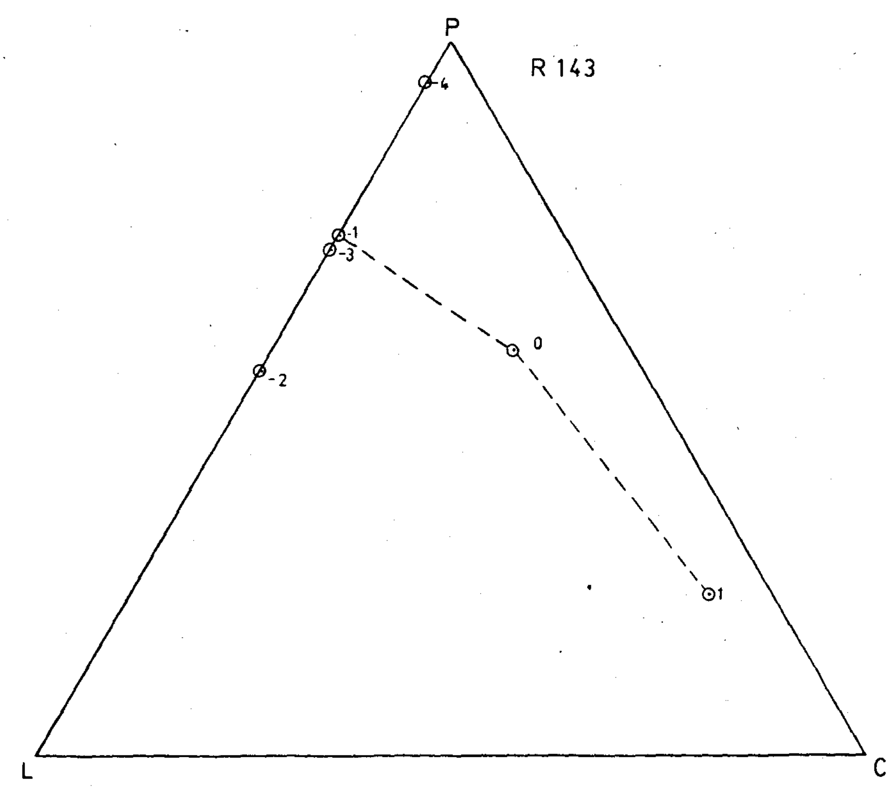
P
R 143
-4
-1
-3
0
-2
1
L
C

Figures 24 to 26. Triangular diagrams for medial samples (R 086 proximal) showing proportions of pumice (P), lithics (L), and crystals (C) at different grain sizes.

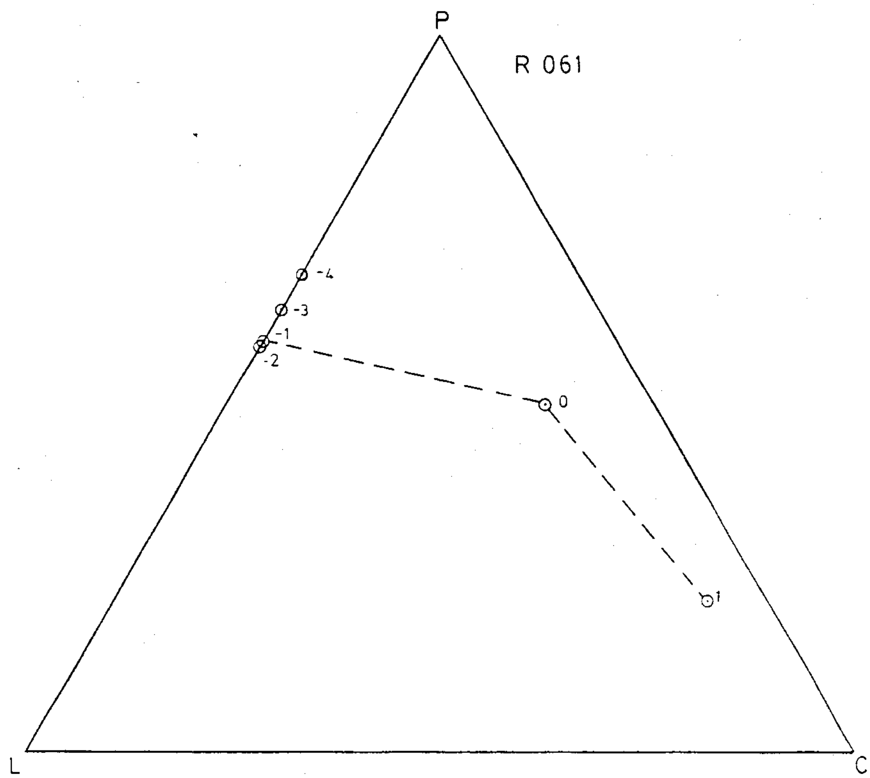
P
R 061
-4
-3
-1
-2
0
1
L
C

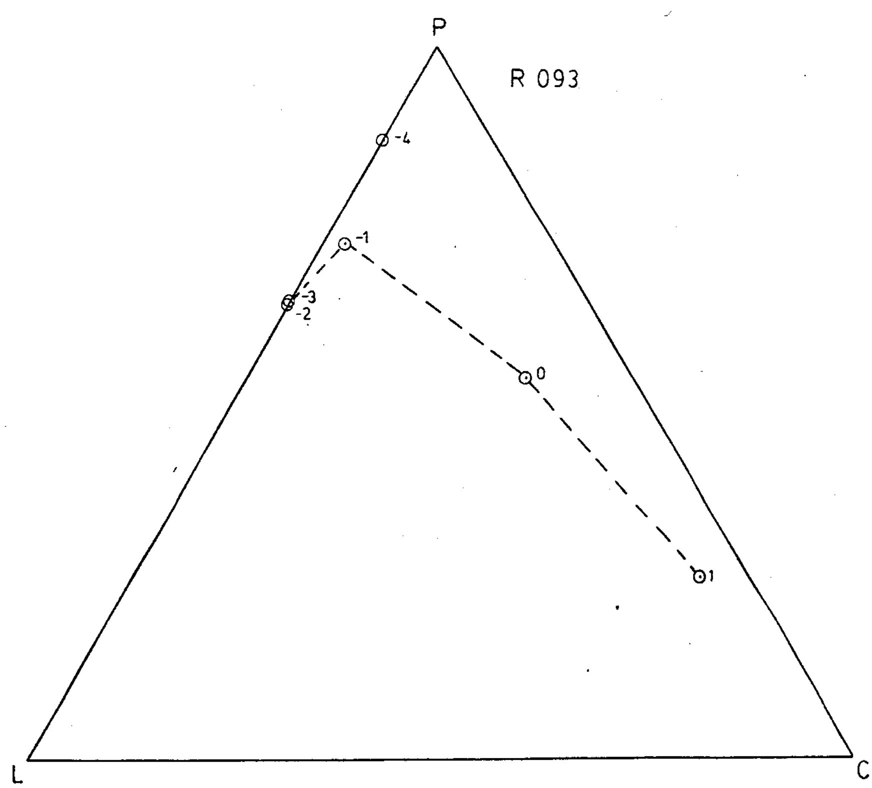
P
R 093
-4
-1
-3
-2
0
1
L
C

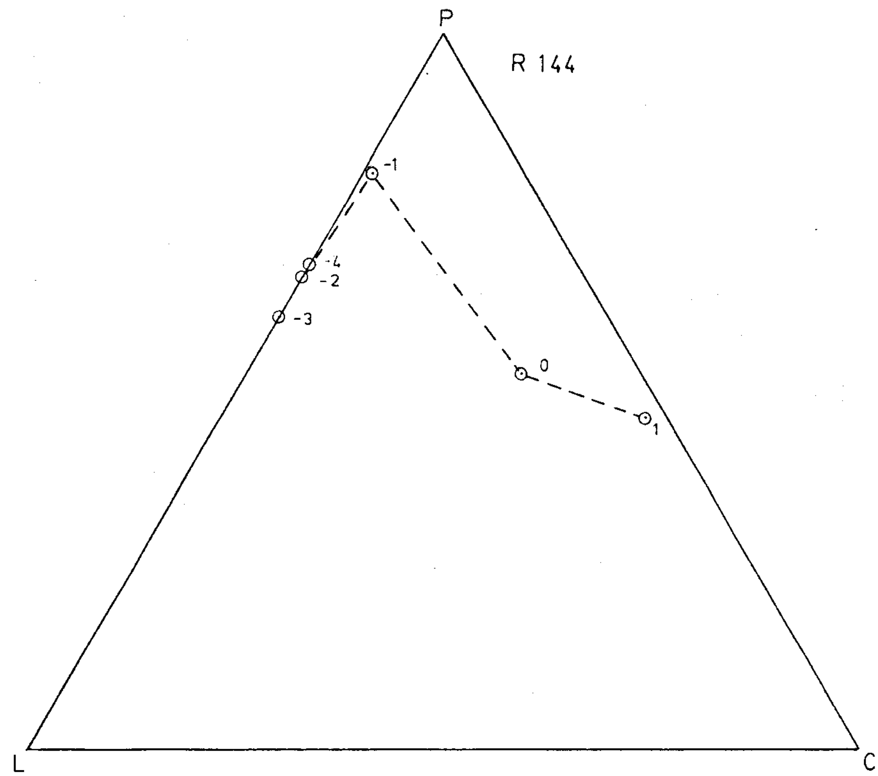
P
R 144
-1
-4
-2
-3
0
1
L
C

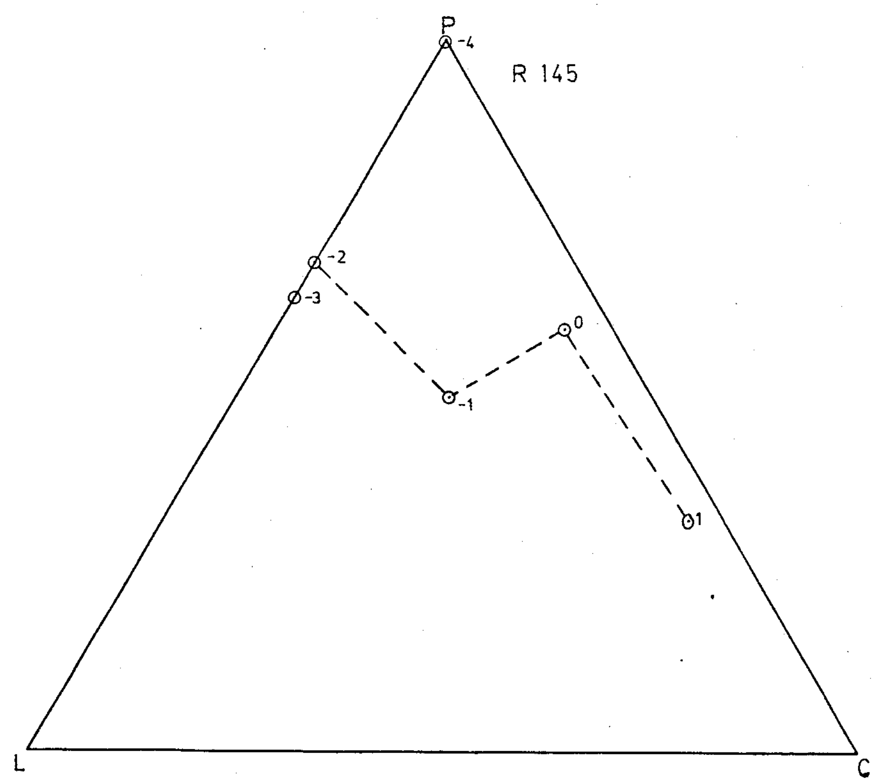
P
-4
R 145
-2
-3
0
-1
1
L
C

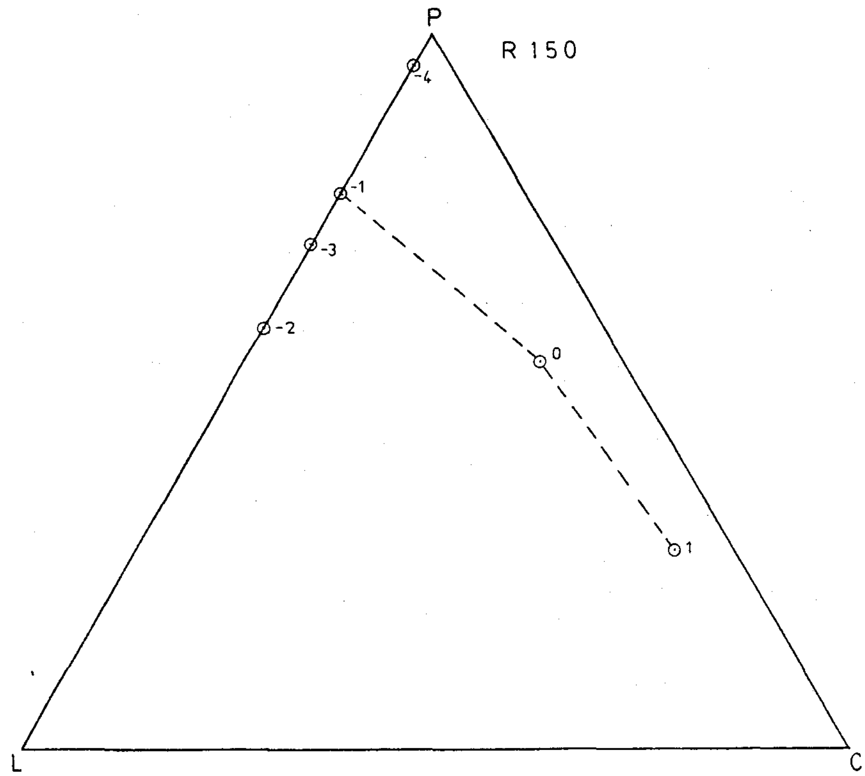
P
R 150
-4
-1
-3
-2
0
1
L
C

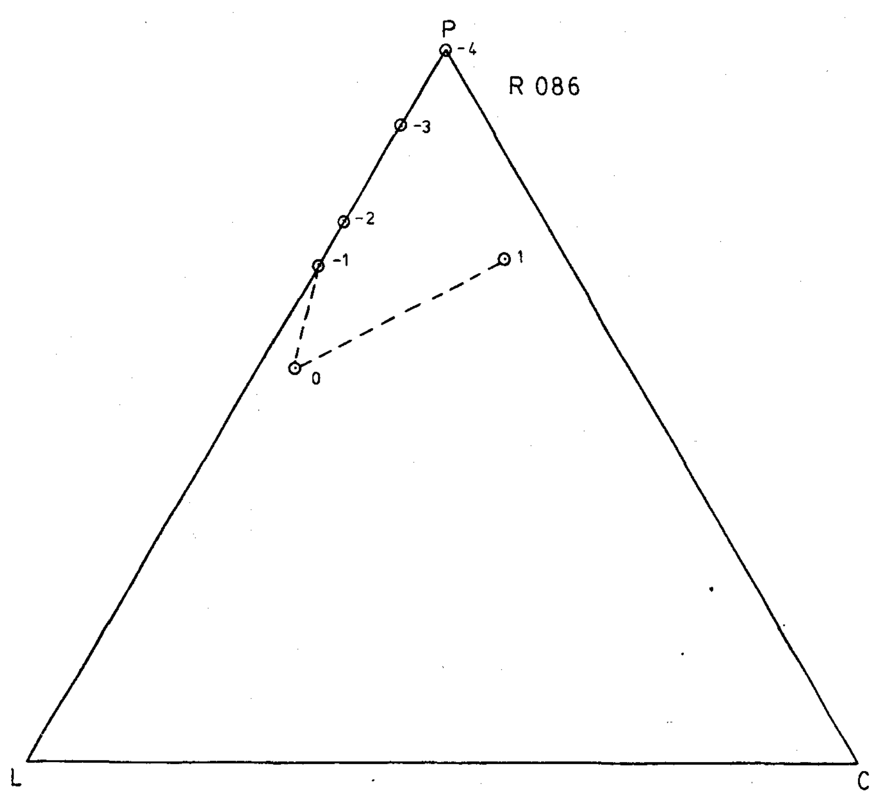
P
-4
R 086
-3
-2
-1
1
0
L
C

Figures 27 to 30. Triangular diagrams for proximal samples showing proportions of pumice (P), lithics (L), and crystals (C) at different grain sizes.

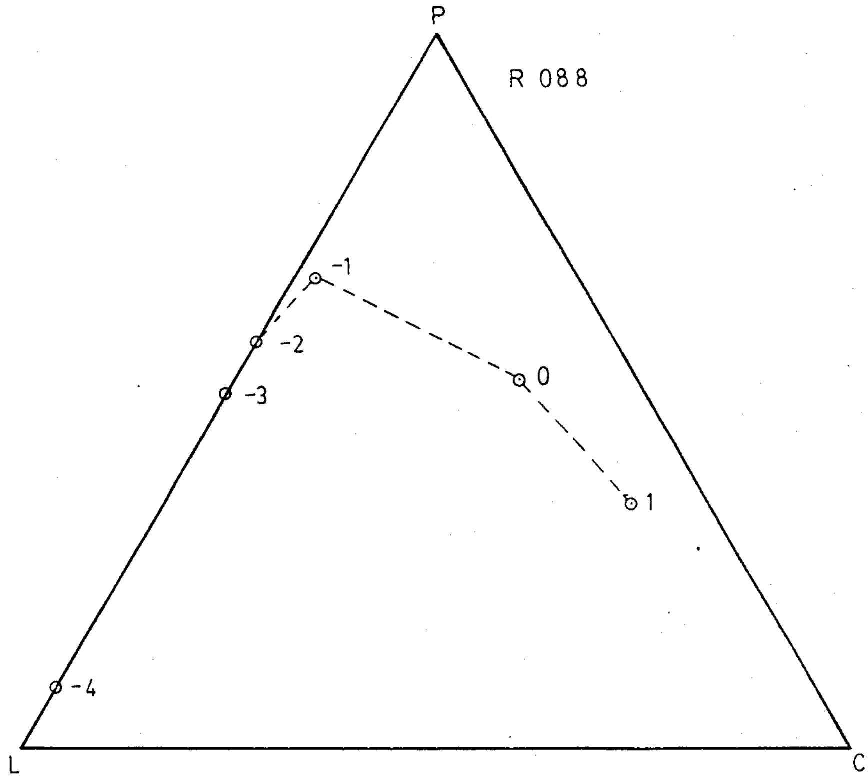
P
R 088
-1
-2
0
-3
1
-4
L
C

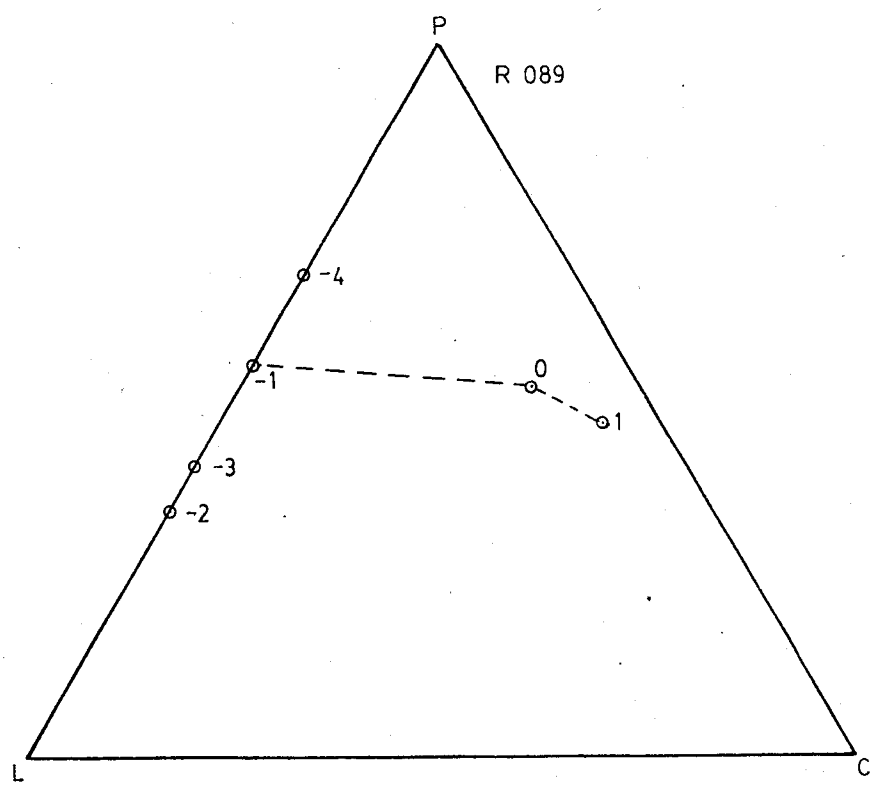
P
R 089
-4
0
-1
1
-3
-2
L
C

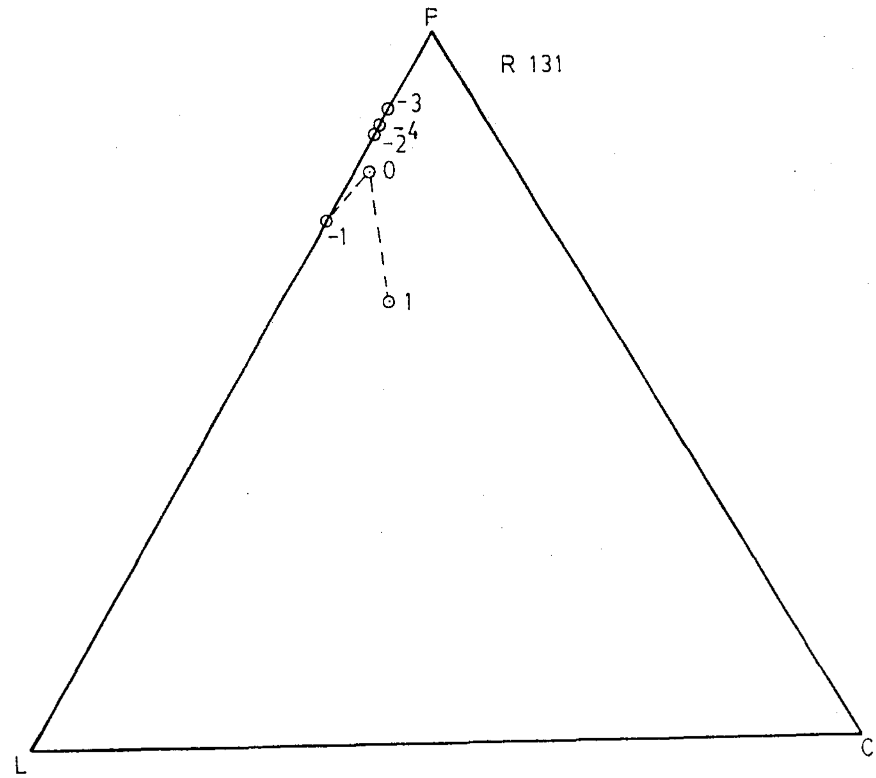
P
R 131
-3
-4
-2
0
-1
1
L
C

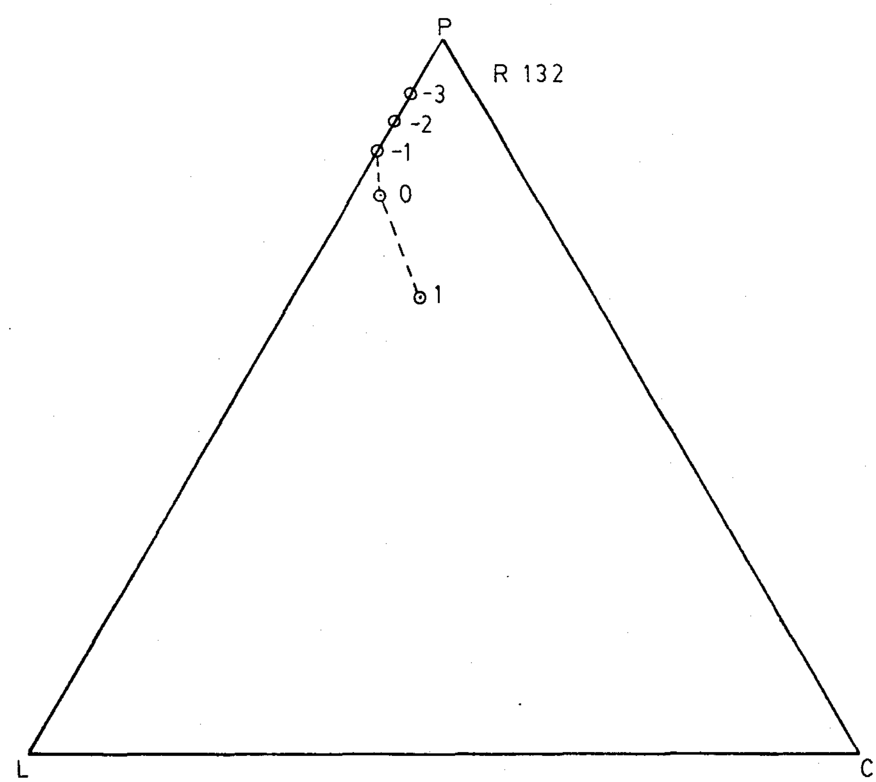
P
R 132
-3
-2
-1
0
1
L
C

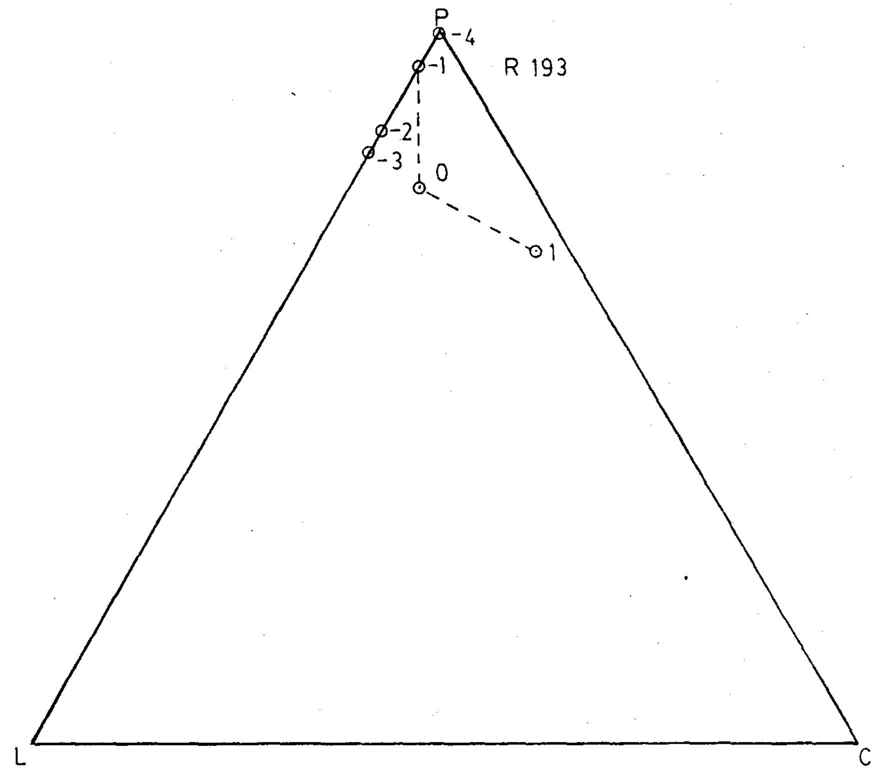
P
-4
-1
R 193
-2
-3
0
1
L
C

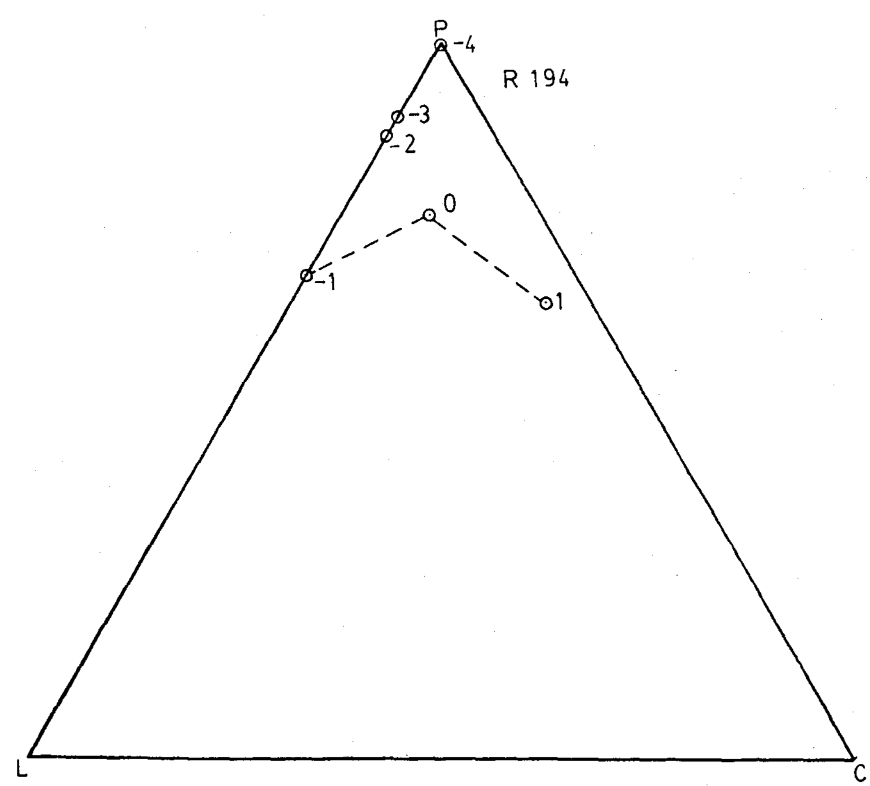
P
-4
R 194
-3
-2
0
-1
1
L
C

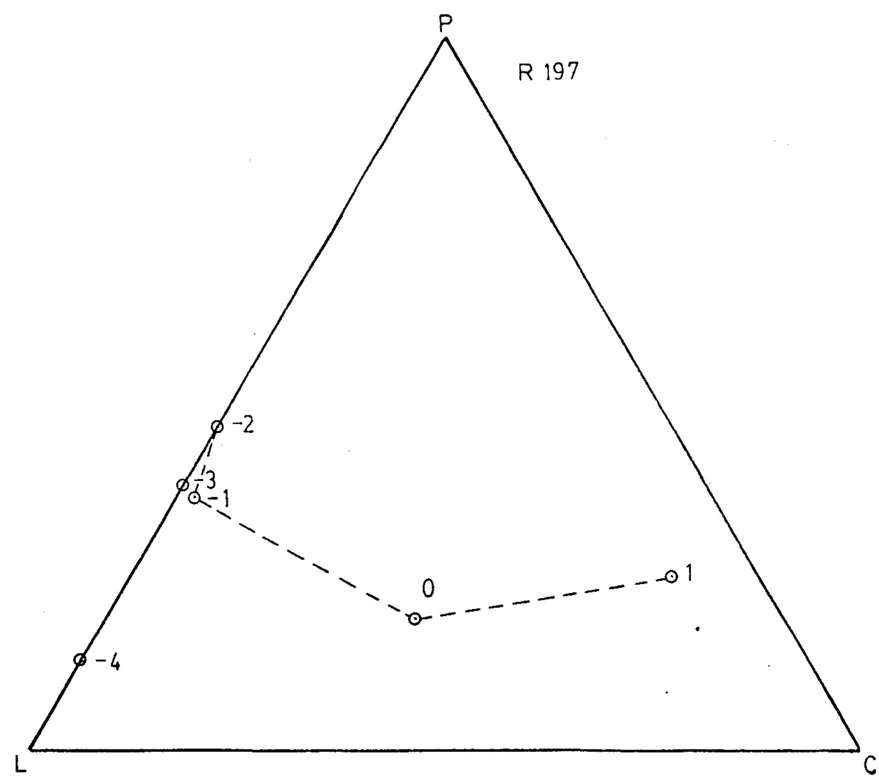

P
R 197
-2
-3
-1
0
1
-4
L
C

Figure 31. Histograms for distal samples in which the bars are subdivided into the correct portions of pumice (stippled), lithics (shaded), and crystals (blank).

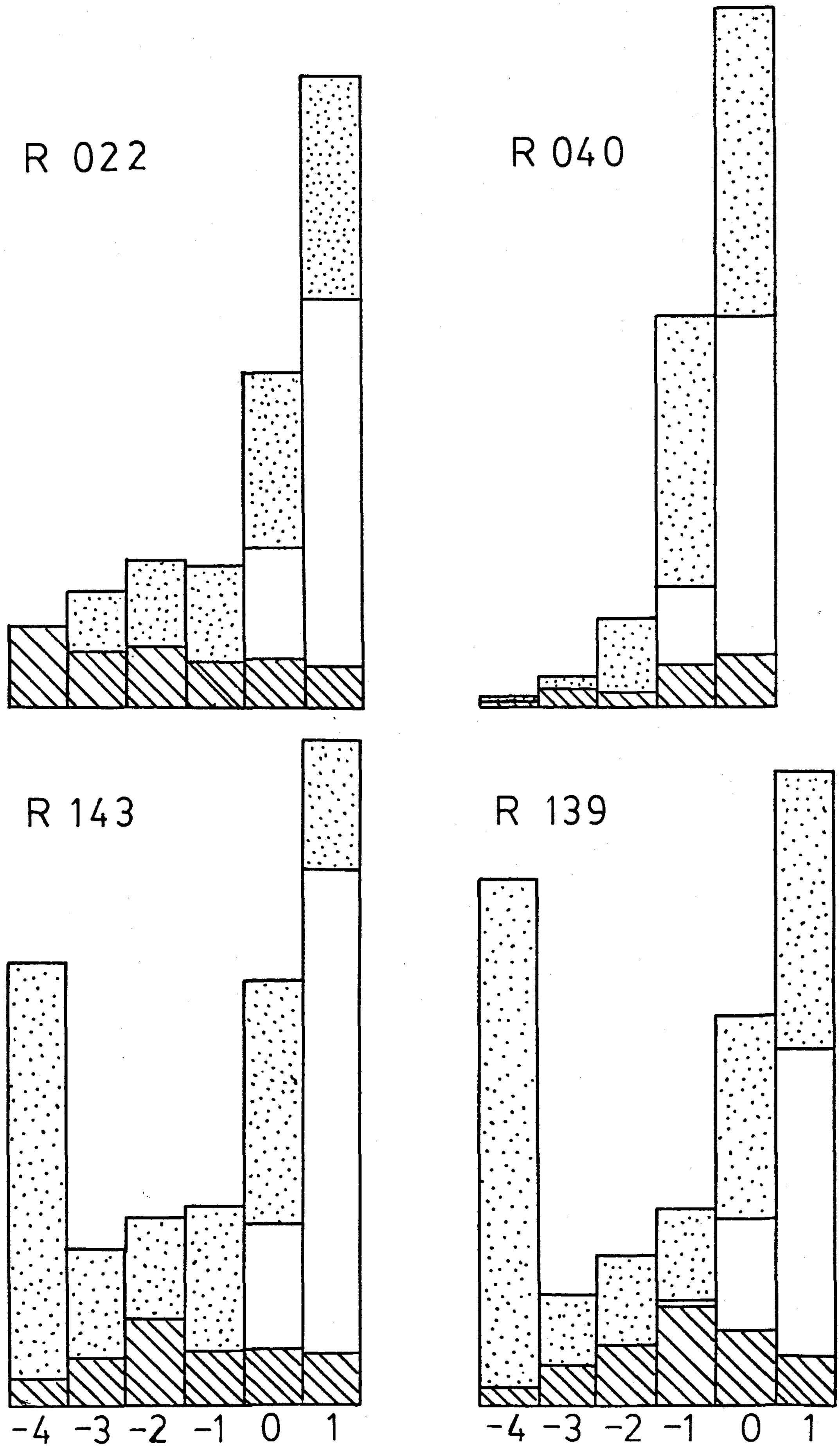

R 022
R 040
R 143
R 139
-4 -3 -2 -1 0 1
-4 -3 -2 -1 0 1

Figure 32. Histograms for medial samples in which the bars are subdivided into the correct proportions of pumice (stippled), lithics (shaded), and crystals (blank).

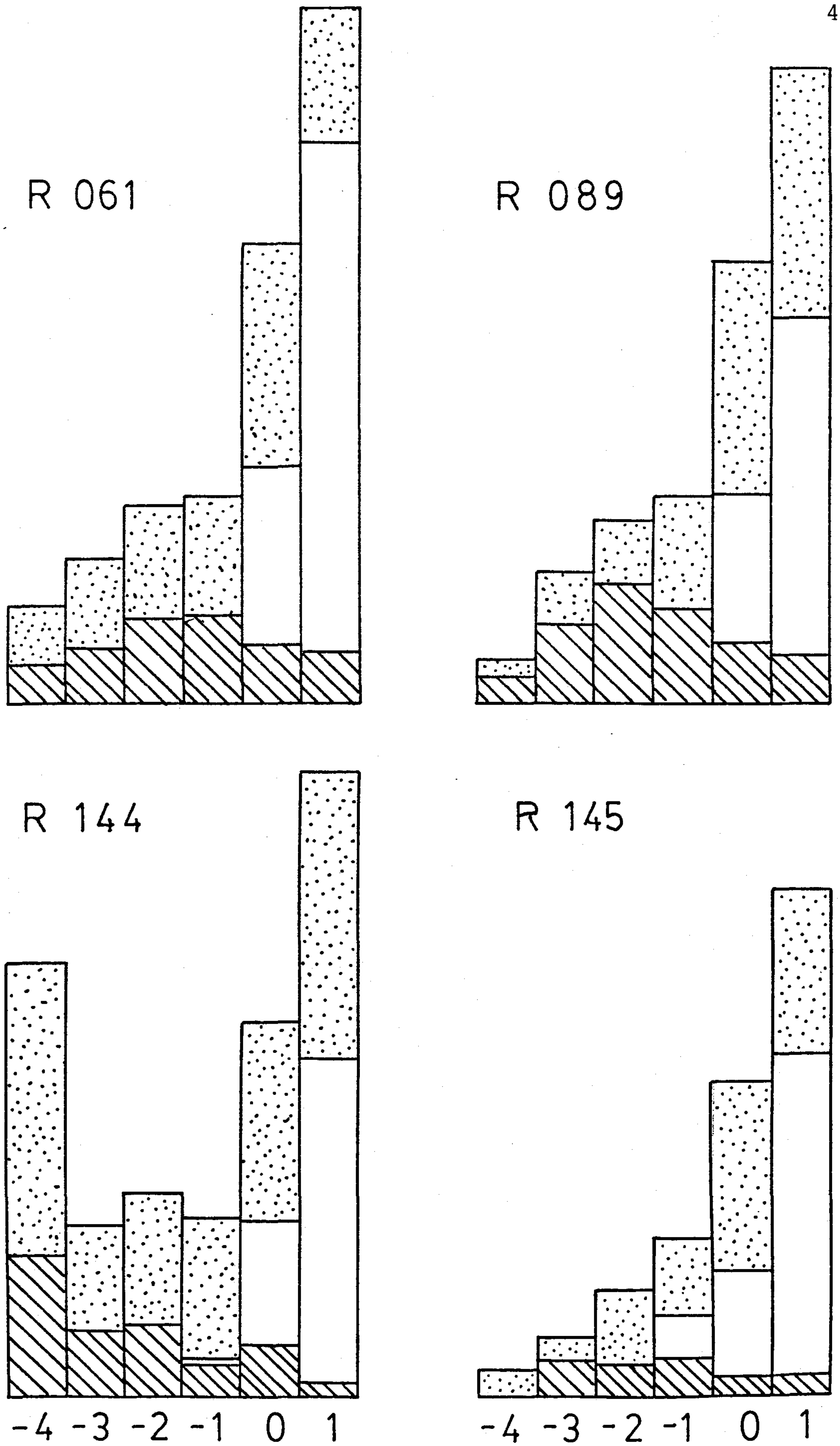
R 061
R 089
R 144
R 145
-4 -3 -2 -1 0 1
-4 -3 -2 -1 0 1

Figures 33 to 34. Histograms for proximal samples (R 150 medial) in which the bars are subdivided into the correct proportions of pumice (stippled), lithics (shaded), and crystals (blank).

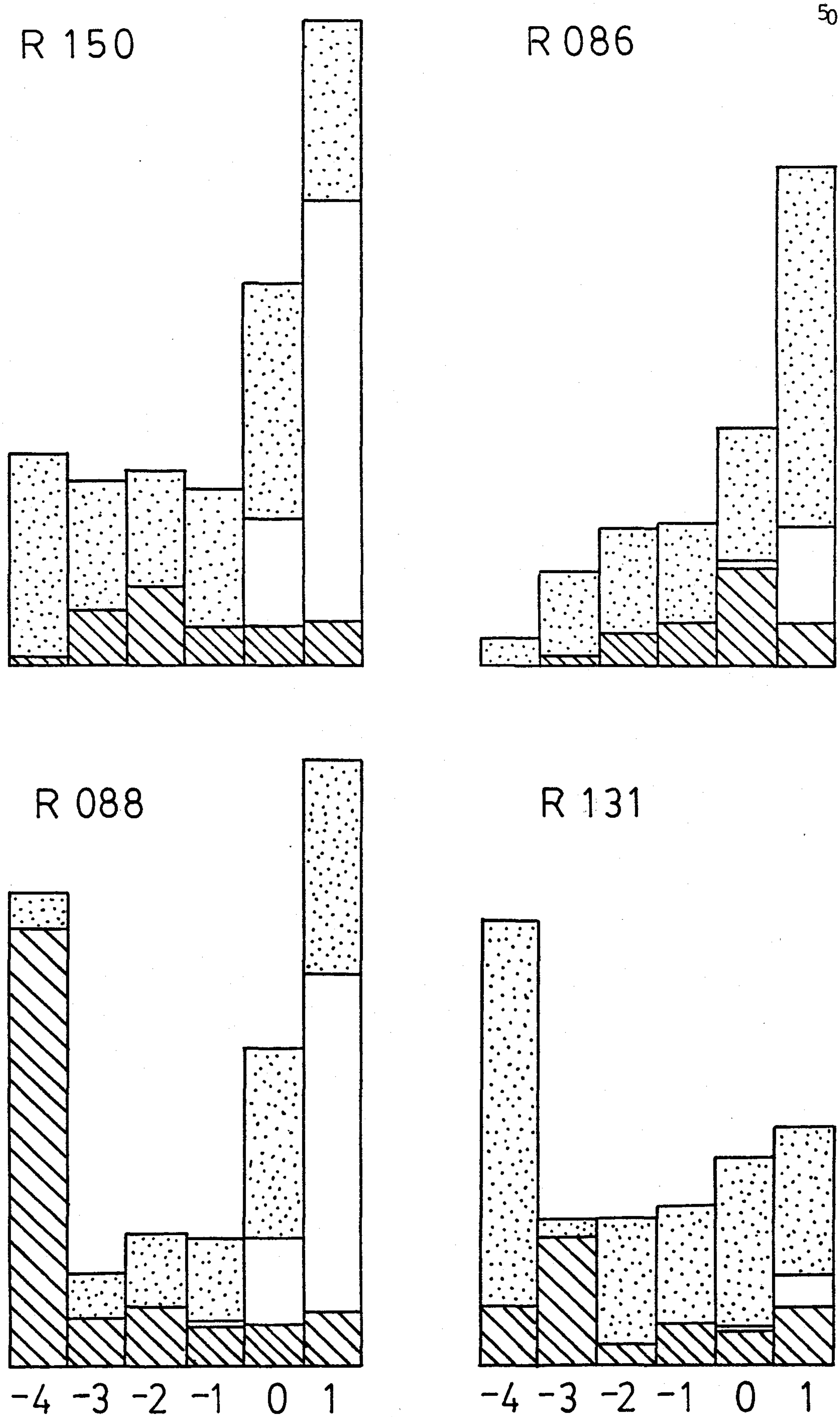
R 150
R 086
R 088
R 131
-4 -3 -2 -1 0 1
-4 -3 -2 -1 0 1

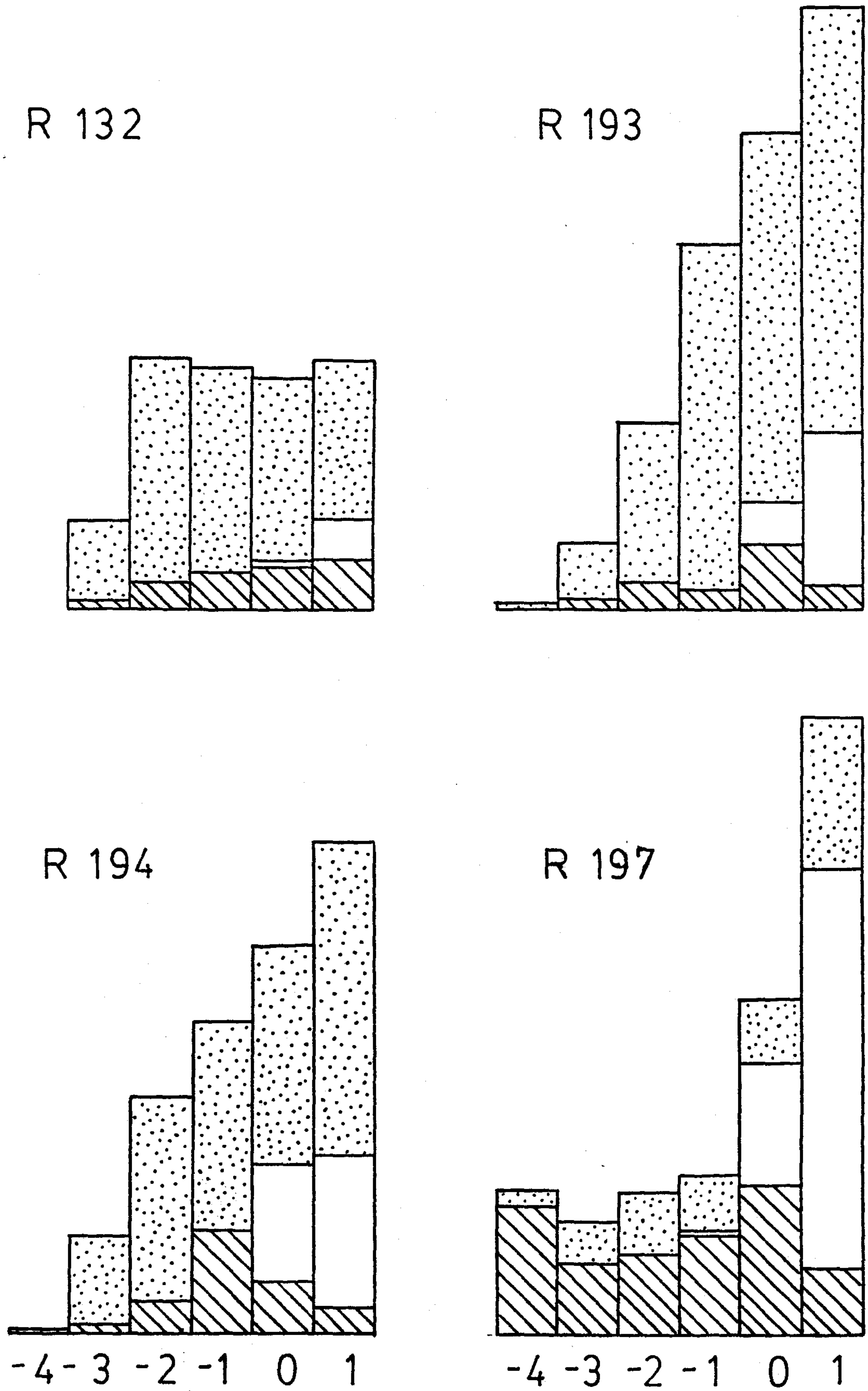
R 132
R 193
R 194
R 197
-4 -3 -2 -1 0 1
-4 -3 -2 -1 0 1

CHAPTER V

INFERENCES

1. NATURE OF THE FLOW

As noted above, the MdØ vs σØ plot produced for the samples in this study fall in the middle of Walker's (1971) flow field (see fig. 21). This is not an exactly definitive method for determining if the deposit is a pyroclastic flow or fall, but it does support the field observations of Clifford (personal communication) and others (e.g. Nairn, 1972).

The lack of differentiation in median grain size and sorting between proximal and distal areas shows that the flow is very homogenous. This leads to the conclusion that no mechanism such as hydraulic sorting existed in the flow to significantly increase sorting with distance travelled. Sparks (1976) has determined that many pyroclastic flows may in fact be laminar or partly laminar in their movement. This was determined by estimating apparent flow viscosities, velocities, and densities, and measuring flow thicknesses in order to obtain a Reynolds number. A laminar flow, by definition, means that different layers of the 'fluid' slide smoothly past one another with little particle diffusion between layers. Thus, little sorting can occur in such an environment. As expected, the sorting values determined for the Rotoiti Breccia are high. Sparks (1976) attributes this to a high particle concentration within the flow rather than any kind of turbulence.

The most interesting feature found in examining the cumulative curves was the bimodal characteristics of the proximal grain populations vs the unimodal characteristics of the medial/distal grain populations. The bimodal population is defined by a break between two adjacent straight line segments, usually at approximately 2Ø, on the probability paper. In general, a bimodal population may be related to (1) nature of the source, (2) mechanical breakage, and (3) hydraulic sorting (Middleton, 1976). The last is immediately discounted since it has already been determined (above) that hydraulic sorting is not a significant factor in this environment. The first is less easily discounted since a bimodal population in a sedimentary environment may reflect its source. However, this is probably not the case here, since the distal and medial populations should also be bimodal and are not. The most plausible explanation then is mechanical breakage. The predominant component of the flow, pumice, is a very fragile material and is easily susceptible to breakage. While carrying out the component analysis, it was observed that the pumice from proximal areas had more angular edges and a lower degree of roundness than the pumice from distal and medial areas. Even though the flow may be partly laminar, there will still be a degree of internal friction and abrasion, and the more time a particular grain spends in the flow, the more rounded and smooth it will become. The break point for most of the proximal curves is at 2Ø (or ¼mm.) which indicates that mechanical breakage falls off below this point and the fines produced by the rounding process begin to dominate. The fact that the bimodal populations are only found in the proximal areas indicates that mechanical breakage is most important at the start of the flow which would produce more grain contact and hence breakage. Sparks (1976) states that "Turbulence is most likely in the early stages of the flow where the flow may be highly inflated and travelling the fastest. As the flow deflates, the increasing viscosity and strength and decreasing thickness and velocity will result in laminar flow developing." With more laminar flow, breakage decreases and the fine population is partly elutriated out resulting in the uni-modal pupulations found in the distal and medial areas.

Pumice is the most important component of the flow because of the nature of the source: the rapid eruption and quenching of a magma does not allow time for any crystallization (excepting that proportion already crystallized) and thus, glass in the form of pumice results. The maximum size of pumice in the Rotoiti Breccia is on the order of 10 to 12 cm. This is controlled by two factors, the initial size of the pumice produced by the sudden magma quenching and the amount of breakage produced by the eruption and subsequent flowage. Pumice is the most important component at the largest grain sizes down to about 1 to 2 mm. This is because it is the most important component overall and the other two components do not occur in significant amounts at these sizes.

The size of crystals found in the deposits is predetermined by the size to which phenocrysts grow in the magma prior to eruption. The largest crystals found are on the order of 1 mm. and this is taken as the limit to the growth size of phenocrysts. Although almost all of the crystals examined were broken, enough of any particular grain was left to allow the determination of its original size. Breakage is also a factor in controlling crystal size, but is nowhere near as important as source. In all of the samples, crystals are the most prevalent at the smallest grain sizes and this occurs for two reasons. Firstly, there was a fairly high number of phenocrysts in the magma to begin with, and secondly, there has been a significant amount of pumice of comparable size lost through elutriation. Gases liberated from and incorporated into the flow rise through the flow and selectively remove pumice because of its lower denisty. The smaller the grain size, the more easily it is removed. Walker (1972) has shown that this process may result in a tenfold concentration of crystals "since loose crystals are present in too high a proportion to be accounted for by the simple fragmentation of magma or pumice." This study shows a comparable degree of crystal concentration overall, but this increases in magnitude from proximal to distal areas. This is almost certainly the product of increasing degrees of elutriation as there is no fresh production of crystals in the flow, only crystals liberated. The main factor is time rather than rate of elutriation since the rate will in fact decrease as the flow progresses (discussed later). Simply put, the material in distal areas has travelled further and longer than material in proximal areas and thus, more pumice has been lost.

The size of lithics is more difficult to deal with since there is not a good control of source. The maximum size of lithics is probably related to the energy of eruption for lithics derived from the vent and magma chamber walls and the energy of flow for lithics incorporated into the flow from the ground. The maximum lithic size found in the Rotoiti Breccia is on the order of 5 to 6 cm. and lithics reach their peak in importance around 4 to 8 mm.

2. NATURE OF THE FLOW

In order for the motion of a pyroclastic flow to be maintained, some degree of fluidization must exist. This greatly decreases frictional resistance and allows the mass of material to be acted on by gravity, even on a shallow slope. The topography over which the Rotoiti Breccia travelled is quite shallow, a slope of approximately 1 degree, so some degree of fluidization must exist for the flow to travel 25 to 30 km.

Experimental studies on fluidization by Wilson (1980) have shown that "With materials having both a wide grain size variation and irregular shape... The grain size variation is so large that the material can never be fully fluidized in the strict sense; before the largest particles are supported, the smallest particles are being lost by elutriation." Thus, pyroclastic material displaying these characteristics will only be partly fluidized, and the larger clasts are supported by the smaller fluidized particles because of a high particle concentration within the flow (Sparks, 1976).

During the course of the flow, fines are continually being created by mechanical breakage and rounding of clasts and then lost through elutriation. In general, the cumulative curves derived for the Rotoiti Breccia samples show a high percentage of fines. This may reflect a greater rate of production of fines than loss of fines, although there is no standard population to which these may be compared.

Evidence for the production of fines from larger particles is the observed rounding of pumices and smoothness of their surfaces. It was noted that both pumice rounding and surface smoothing increased with increasing distance from source. This indicates that there was continual production of fines while the flow was in motion, through the process of abrasion.

Evidence of elutriation of pumice fines is the degree of crystal enrichment relative to the 'standard' crystal content of a pumice fragment. This too, increased with increasing distance from source indicating continual loss of fines while the flow was in motion. Further evidence of elutriation is the highly turbulent cloud of fine material actually observed over moving pyroclastic flows.

It is not possible to derive relative rates of production and loss of fines by measuring grain roundness or degree of crystal enrichment. However, by examining the form of the plotted cumulative curves, some idea of which process was more important may be determined.

It seems reasonable that the most important breakage mechanism is the smoothing by attrition of the surfaces of pumice clasts producing fine material directly rather than breaking each pumice fragment in half indirectly producing fine material. It is further postulated that this process is most effective at larger grain sizes and negligible at fine grain sizes.

A model based on these criteria was developed where 10% by weight of larger pumice grain sizes was 'lost' and distributed in a log-normal fashion among the finer grain sizes. It was found that if a closed system was considered, any particular cumulative curve would be steepened in slope. The population would be better sorted and the median grain size would decrease slightly. If larger percentages of pumice were removed, these effects became more pronounced. With an open system, fine material is lost and the curve does not steepen as much. The sorting does not improve as much and the median grain size does not decrease as much.

Upon examination of the form of the curves, it is found that the medial/distal curves do steepen somewhat compared to proximal curves. This is a very general trend as in some individual curves, this trend may be reversed. The rate of production of fines must have been greater than the rate of elutriation since the curves do steepen, but not a great deal. This conclusion is reinforced by the high proportion of fine material found throughout the flow deposits.

As the flow progressed to distal areas, its ability to transport material was lessened. This is best shown by the gradual decrease in maximum lithic clast sizes further from the source area. Part of the reason is that the slope of the volcano decreases slightly, from 1 degree to ½ degree towards the Bay of Plenty. However, the main reason probably lies in a decreasing degree of fluidization. As shown above, there is no shortage of fine material to be fluidized so the amount of gas driving the process must have decreased. There are two principle gas sources. Internally, gas is released from juvenile clasts by diffusion or breakage, while externally, gas may be initially trapped in the material or incorporated into the flow at its head (Wilson, 1980). Of these, both Wilson (1980) and Sparks (1976) consider the gas released by diffusion from juvenile clasts to be the most important in maintaining fluidization. As the flow progresses, the gas concentration in the clasts will decrease and the rate of diffusion will fall off. As a consequence, the degree of fluidization in the flow must decrease as must the flow's ability to transport material. Eventually, increasing friction combined with a shallower slope brought the whole process to an end.

CHAPTER VI

PHENOCRYSTS

All crystalline phases found in a pyroclastic deposit are derived from the magma prior to eruption, as the eruption process itself is too rapid to allow ordered structures to form. The crystals, therefore, reflect conditions within the magma chamber rather than within the flow.

The major phases occuring in the Rotoiti Breccia are quartz, plagioclase feldspar, and alkali feldspar (sanidine). The minor phases include amphibole (cummingtonite), iron oxide (magnetite), and biotite. The feature noted in all crystals observed was euhedralism which indicates crystal growth into free space.

Quartz is the most prevalent mineral phase indicating a rhylitic composition. This is confirmed by a chemical analysis of ignimbrites in the area by Ewart and Stipp (see table 3). It is the most important crystalline phase at 1 mm., but decreases in importance at smaller grain sizes because of larger quantities of other minerals. All of the quartz has a bipyrimidal crystal form which is typical of beta-quartz. Below the alpha-beta inversion of quartz, only alpha quartz exits, so this relic crystal form shows the temperature of the magma must have been greater than 573^{o}C when the quartz was formed.

There are two kinds of feldspar present, sanidine and plagioclase. The plagioclase displays spectacular oscillatory compositional zoning (see fig. 35) indicative of a complex crystallization process.

Each crystal with zoning has undergone continuous crystallization, but under varying pressure and temperature regimes. This is best equated with a few cycles of vertical movement of the crystal within the magma chamber before eruption. The high temperature alkali feldspar sanidine is indicative of the magma's high temperature, and the suddeness of the extrusion. The feldspars are the dominant crystalline component at ½ mm.

The minor phases, cummingtonite, magnetite, and biotite, all generally occur at grain sizes below ¼ mm. Ewart (1968) has pointed out that the Rotoiti Breccia differs significantly from other acid volcanic rocks in the area in that it contains cummingtonite instead of calcic hornblende. Cummingtonite has only been recognized as an acid volcanic phenocryst rather than a metamorphic mineral in the past 15 years (Carmichael et al, 1974). An example of a cummingtonite crystal within a pumice fragment is shown in figure 36. The presence of magnetite rather than hematite shows the system lies below the hematite-magnetite buffer, however, no specific temperature can be assigned to the magma since the amount of oxygen in the system is not known.

Figure 35. Photomicrograph showing oscillatory zoning in plagioclase. Crossed polars.

Figure 36 Photomicrograph showing cummingtonite and magnetite in pumice. Partially crossed polars.

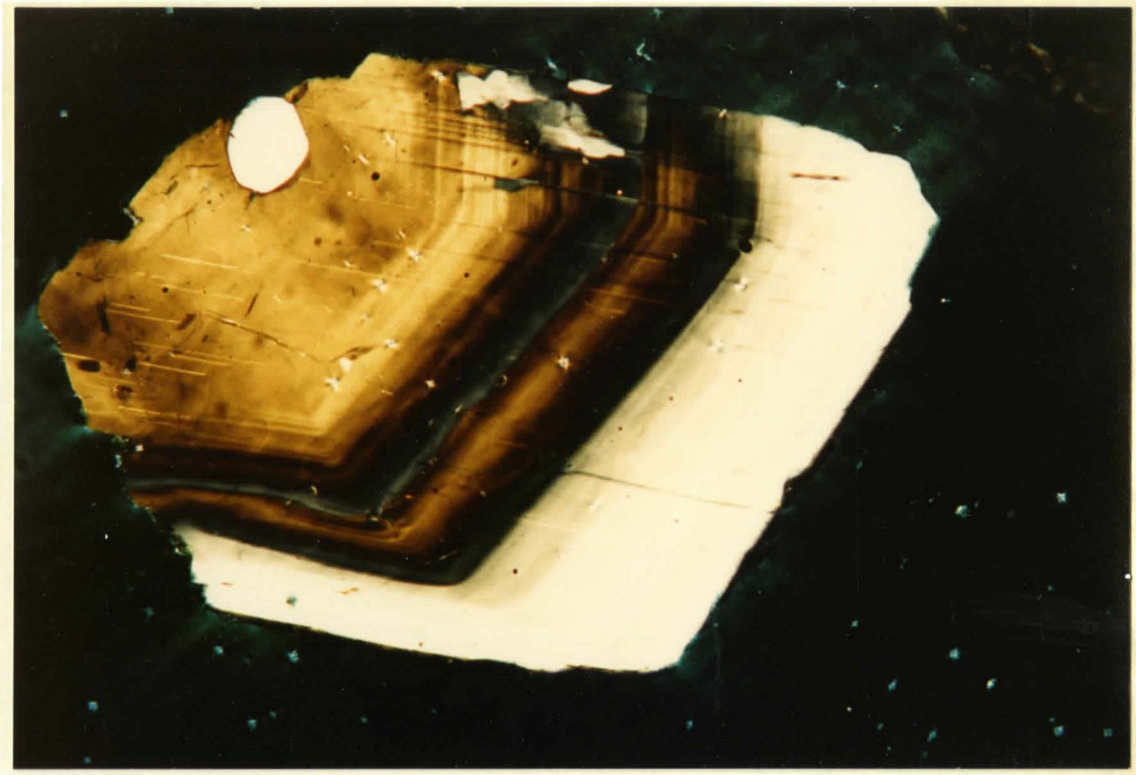

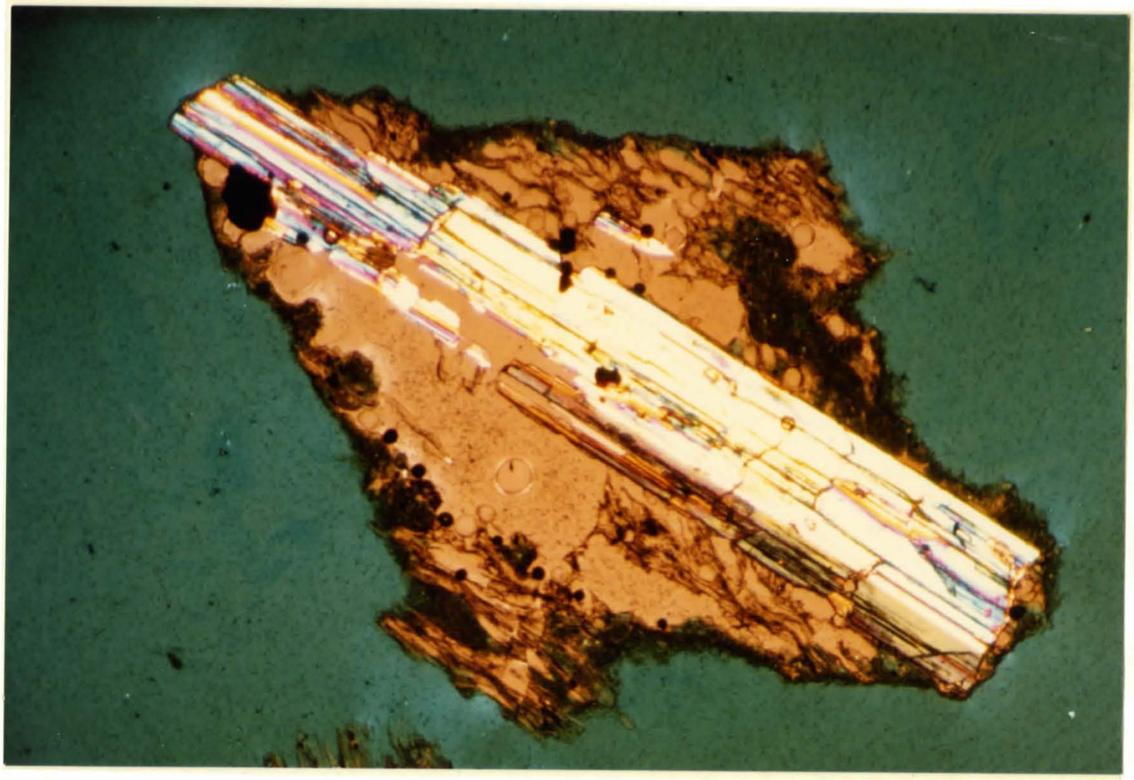

TABLE 3

	1	2
SiO_2	74.22	73.85
Al_2O_3	13.27	13.55
Fe_2O_3	0.88	1.25
FeO	0.92	0.60
MgO	0.28	0.30
CaO	1.59	1.53
Na_2O	4.24	3.71
K_2O	3.18	3.60
TiO_2	0.28	0.23
P_2O_5	0.05	0.05
MnO	0.05	0.05
H_2O^+	0.80	0.59
H_2O^-	0.23	0.38
CO_2	---	---

1. Average composition of rhyolite lavas and domes (average of 25 analyses).
2. Average composition of ignimbrites (average of 17 analyses) [Ewart and Stipp, 1968]

CHAPTER VII

VESICULATION AND BUBBLE SHAPE

To examine the bubble shape of the pumice fragments, a thin section mount of a few pumice grains was prepared. The pumice was placed in an epoxy and cut when it hardened so the bubbles are highlighted by the epoxy's distinct blue colour (see figs. 37 & 38).

All of the pumice grains examined in this manner had a very high number of bubbles occupying approximately 60 to 70% of the pumice by volume. This indicates that that portion of the magma erupted was very highly vesiculated and implies a pumice density of about 0.8 g/cc. It is generally considered that the process of volatile exsolution and bubble disruption is the principle driving mechanism of a violent pyroclastic eruption. The growth of bubbles in a magma is controlled by two processes; diffusion of gas dissolved in the magma and decompression of the gas as pressure in the magma decreases. Decompressional growth is dominant for large bubbles and for all bubbles at low pressures (Sparks, 1978). Under high pressure, volatiles are dissolved in the melt, but as the melt rises to the surface, the hydrostatic pressure decreases causing the volatiles to exsolve into a vapour phase. A point is reached where the bubble population has increased to a level where no further expansion can occur because of crowding. However, gas continues to diffuse into the bubbles as pressure equilibrium is not yet reached and the internal pressure builds. Eventually, the magma disrupts because of the large pressure gradient between the gas in the bubbles and gas above the melt surface, producing an explosive eruption (Sparks 1978). The high vesicularity and thin walls of the pumice indicates that such a process was responsible for the eruption producing the Rotoiti Breccia, since the internal structure of the pumice represents the condition of the magma just prior to eruption.

A dominant feature seen in all of the pumice examined is the drawn out nature of the gas bubbles. Axial ratios of the bubbles approximate 4:1:1 making them elliposoidal rather than spheroidal. Under static conditions, a bubble should grow as a sphere because of constant surface tension. Thus, the elongated bubbles must be the product of flowage in the magma;--most likely occuring during the initial part of the eruption, where the viscosity of the melt has increased somewhat, but has not yet solidified. The drawn out bubbles are the controlling factor of the shape of pumice shards (noted earlier).

Figure 37. Photomicrograph showing drawn out gas vesicles in pumice. Plane polarized light.

Figure 38. Photomicrograph showing drawn out gas vesicles in pumice and a zoned plagioclase phenocryst. Partially crossed polars.

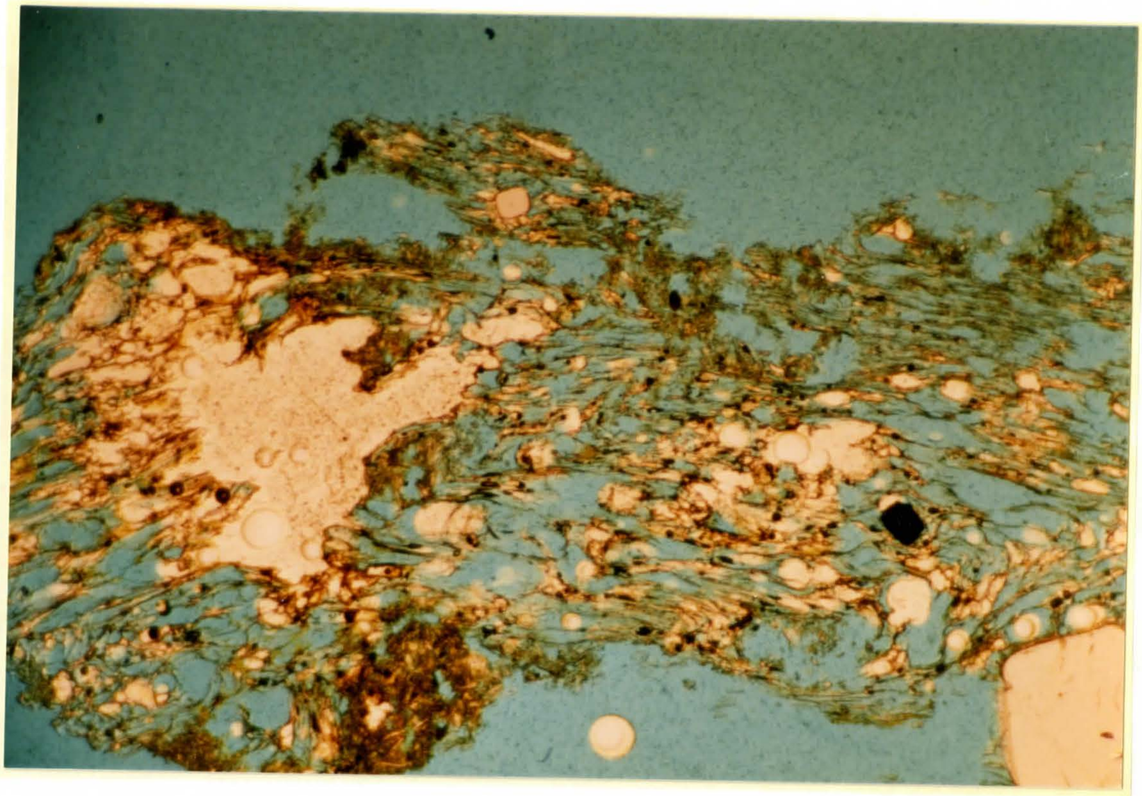

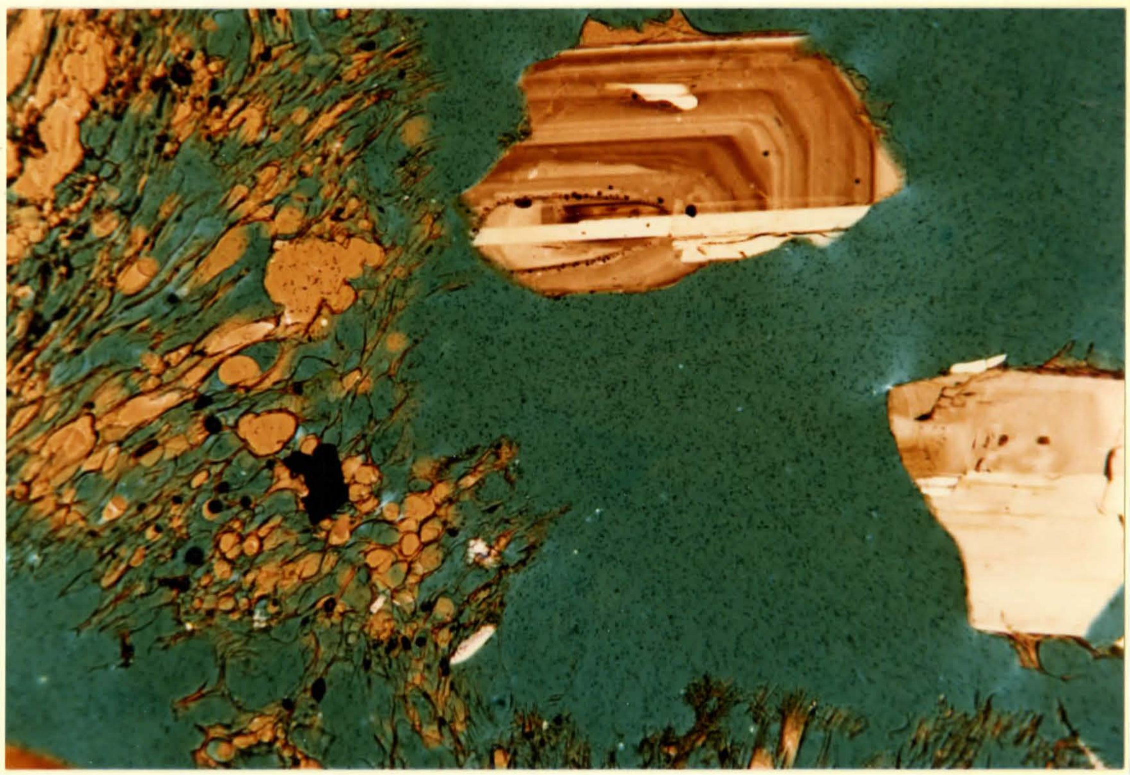

CONCLUSIONS

The Rotoiti Breccia Formation was deposited as a pyroclastic flow from a fairly low energy eruption. The low energy of the eruption, and hence of the flow, has constrained the formation to the topographic low between two underlying ignimbrites. Either erosion of actual draining of the material has resulted in the formation's stratigraphical discontinuity with its source.

In order for the flow to travel 30 km. over a shallow slope, it must have been partly fluidized by gas released from juvenile pumice clasts. As a consequence, abrasion and elutriation of pumice fines during the flow's movement has resulted in a significant amount of crystal enrichment in distal areas of the flow as compared to proximal areas.

Sorting and median grain size do not change significantly from proximal to distal areas because of the laminar nature of the flow; the surficial abrasion will not greatly affect these quantities. The high particle concentration of the flow allows it to carry large clasts which are not fluidized, however, this ability is decreased as the flow progresses. At the very beginning of the flow, more turbulence is present and mechanical breakage is significant. This results in the bimodal cumulative curves for proximal areas as opposed to the unimodal curves for distal areas.

BIBLIOGRAPHY

CARMICHAEL, I.S.E., TURNER, F.J., VERHOOGEN, J., 1974. Igneous Petrology. McGraw-Hill Book Co. , New York, 1-739.

EWART, A., 1968. The Petrography of the Central North Island Rhyolitic Lavas, Part two. Regional Petrography Including Notes on Associated Ash-Flow Pumice Deposits. N.Z.J. Geol. Geophys. vol. 11, 478-545.

EWART,AA., and STIPP, J., 1968. Petrogenesis of the Volcanic Rocks of the Central North Island, New Zealand, as indicated by a study of Sr 87/Sr 86 ratios and Sr, Rb, K, U, and Th abundances. Geochim et Cosmochim. Acta vol. 32, 128-144.

FISHER, R.V., SCHMINKE, H. -U., 1984. Pyroclastic Rocks. Springer-Verlag., Berlin, 1-472.

GRANT-TAYLOR, T.L. and RAFTER, T.A., 1971. New Zealand Radiocarbon Age Measurements -6. NN.Z.J. Geol. Geophys. vol. 14, 364-402.

HEALY, J., SCHOFIELD, J.C., and THOMPSON, B.N. 1964, Sheet 5, Rotorua (1st Ed.). "Geological Map of New Zealand 1;250,000" Department of Scientific and Industrial Research, Wellington, New Zealand.

KOHN, B.P., and TOPPING, W.W., 1978. Time-Space REIationships Between Late Quaternary Rhyolitic and Anddsitic Volcanism in the Southern Taupo Volcanic Zone, New Zealand. Geol. Soc. Am. Bull. vol. 89, 1265-1271.

KITTLEMAN, L.R., 1964. Application of Rosin's Distribution in Size- Frequency Analysis of Clastic Rocks. J. Sed. Petrol. Vol. 34, 483-502.

KUNO, H., ISHIKAWA, T., KATSUI, Y., YAMASAKI, M., and TANEDA, S., 1964. Sorting of Pumice and Lithic Fragments as a Key to Eruptive and Emplacement Mechanism. Jap. J. Geol. Geog. Vol. 35, 223-238

MARSHALL, P., 1935. Acid Rocks of the Taupo-Rotorua Volcanic District. Trans. Roy. Soc. N.Z. vol. 64, 323-366.

MIDDLETON, G.V., 1976. Hydraulic Interpretation of Sand Size Distributions. J. Geol. vol. 84., 405-426.

NAIRN, I.A., 1972. Rotoehu Ash and the Rotoiti Breccia Formation, Taupo Volcanic Zone, New Zealand. N.Z.J. Geol. Geophys. vol. 59. 251-261.

NAIRN, I.A., and KOHN, B.P., 1973. Relation of the EArthquake Flat Breccia to the Rotoiti Breccia, Central North Island, New Zealand. N.Z.J. Geol. Geophys. vol. 16, 269-279.

ROGAN, M., 1982. A Geophysical Study of the Taupo Volcanic Zone, New Zealand. J.G.R. vol. 87, No. B5, 4073-4088.

SHERIDAN, M.F., 1971. Particle-Size Characteristics of Pyroclastic Tuffs. J. Geophys. Res. vol. 76, 5627-5634.

SPARKS, R.S.J. 1976. Grain Size VAriations in Ignimbrites and Implications for the TRansport of Pyroclastic Flows. Sedimentology. vol. 23, 147-188.

SPARKS, R.S.J., SELF, S., and WALKER, G.P.L., 1973. Products of Ignimbrite Eruption. Geology vol. 1, 115-118.

SPARKS, F.S.J., 1978. The Dynamics of Bubble Formation and Growth in Magmas: A Review and Analysis. J. Volcanol. Geotherm. Res. vol. 3, 1-37.

THOMPSON, B.N., 1968. Age of Rotoiti Breccia. N.Z.J. Geol. Geophys. vol. 11, 1189-1191.

VUCETICH, C.G., and PULLAR, W.A., 1969. Stratigraphy and Chronology of late Pleistocene Volcanic Ash Beds in Central North Island, New Zealand. N.Z.J. Geol. Geophys. vol. 12, 784-837.

WALKER, G.P.L. 1972. Crystal Concentration in Ignimbrites. Contr. Mineral. Petrol. vol. 36, 135-146.

WALKER, G.P.L., 1971. Grain-Size Characteristics of Pyroclastic Deposits. J. Geol. vol. 79, 696-714.

WALKER, G.P.L, SELF, S., and FROGGATT, P.C., 1981. The Ground Layer of the Taupo Ignimbrite: A Striking Example of Sedimentation From a PYroclastic Flow. J. Volcanol. Geotherm. Res. vol. 10, 1-11.

WILSON, C.J.N., 1980. The Role of Fluidization in the Emplacement of Pyroclastic Flows: An Experimental Approach. J. Volcanol. Geotherm. Res. vol. 8, 231-249.